FUNCTIONAL MODULATION OF DBC2 BY THE HSP90 CHAPERONE MACHINE

By

JACOB RAY MANJARREZ

Bachelor of Science in Cell and Molecular biology
Oklahoma State University
Stillwater, Oklahoma
2003

Submitted to the Faculty of the
Graduate College of the
Oklahoma State University
in partial fulfillment of
the requirements for
the Degree of
DOCTOR OF PHILOSOPHY
May, 2012

FUNCTIONAL MODULATION OF DBC2 BY THE

HSP90 CHAPERONE MACHINE

Dissertation Approved:

Dr. Robert L. Matts

Dissertation Adviser

Dr. Andrew Mort

Dr. Ramamurthy Mahalingam

Dr. Stacy Benson

Outside Committee Member

Dr. Sheryl A. Tucker

Dean of the Graduate College

TABLE OF CONTENTS

Chapter Page

LIST OF TABLES

Table Page

LIST OF FIGURES

CHAPTER I

DBC2 Literature Review

The ability of cancer cells to proliferate and metastasize are commonly attributed to deletions and mutations of genes that regulate cellular growth cycles and programmed cell death (PCD a.k.a., apoptosis), or activation or suppression of their expression. These genes commonly fall into two classes: proto-oncogenes that stimulate cell proliferation and tumor-suppressor genes that suppress cell growth.

Deleted in Breast Cancer 2 (DBC2/RhoBTB2) is a tumor suppressor gene that has roles in suppressing cell proliferation and stimulating PCD. DBC2 was first identified through a Representational Difference Analysis (RDA) of human breast tumor biopsies (Hamaguchi et al. 2002). DBC2 was found to be deleted in 3.5% of the tumors assayed but now the expression of DBC2 has been shown to be lost in 60% of samples and has been linked to poor breast cancer prognosis (Hamaguchi et al., 2002; Mao et al., 2010). DBC2 was also identified in a loss of heterozygosity (LOH) screen from bladder cancer samples and is currently known to affect additional tumor and cells line such as lung, ovary, cervical, prostate, colon, rectum, kidney, stomach larynx and head and neck (Wilkins et al., 2004; Siripurapu et al., 2004; Berthold et al., 2008; Mao et al., 2010.) The deletion was mapped to chromosome 8p21.2 with six genes including DBC2 extending from the mapping reference site (Hamaguchi et al. 2002; Ramos et al,

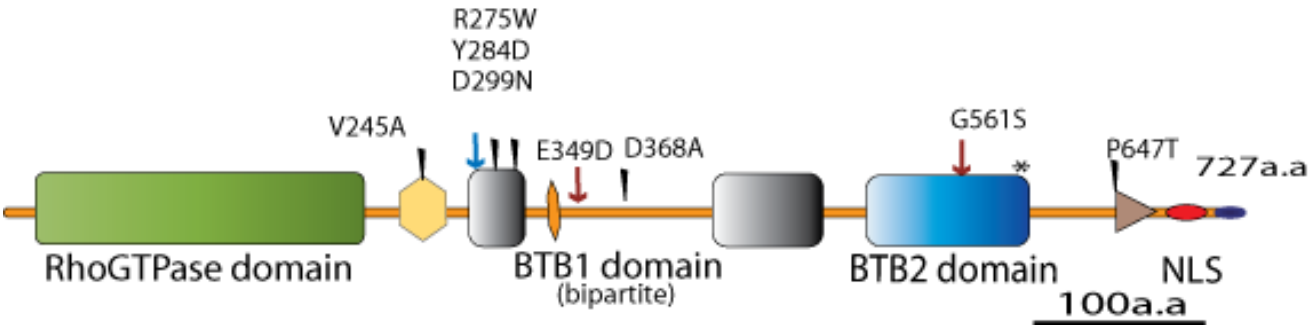

Figure 1: DBC2 domain structure. Major domains are labeled with the Pro rich region containing the PEST motif in yellow, His rich region in orange, NLS in red, and the Ser rich element in dark blue with the putative RING domain transparent brown. Black spikes are the mutations from breast, lung cancer, bladder cancer maroon arrows, and gastric cancer blue arrow. Read from left to right, V245A, R275W, Y284D, D299N, E349D, D368A, G561S and F647T. The asterisk is the breakpoint location indicted by Hamaguchi et al (2002). Domain figure adapted from Aspenstrom et al. (2007).

2002). The deletion focal point was noted to be within intron 7 of DBC2 extending into the 3' untranslated region (UTR) of a neighboring gene (Hamaguchi et al. 2002). The sequence loss at this location would be in excess of ~55% of the total gene coding region.

The DBC2 domain structure was first thought to encode a Ras domain followed by tandem BTB (broad complex/bric-a-brac/poxvirus/zinc finger) domains (Hamaguchi et al. 2002). Upon further analysis the putative guanine nucleotide binding domain of DBC2 was found to be member of the atypical RhoGTPase class of G-protein domains. DBC2 is arranged from the amino-terminal (N-terminal) end as a Rho domain followed by a PEST motif inside of a proline rich region, a tandem pair of broad-complex tramtrack, bric a brac/poxvirus zinc finger (BTB/POZ; referred to as BTB), a C-terminal domain containing a putative ring finger domain with a bipartite nuclear localization signal (NLS), ending with a serine rich region (Figure 1). The first BTB domain has a bipartite arrangement with an approximate 106 amino acid (AA) spacer containing a poly-histidine rich region, a motif that is considered to be a signal for nuclear speckle localization (Salichs et al. 2009).

The gene that encodes DBC2 shows evolutionarily specificity to mammals but include orthologs in *Gallus gallus, Danio rerio*, *Dictyostelium discoideum*, *Drosophila melogaster* and *Anopheles gambiae* (Hamaguchi et al, 2002; Ramos, S., et al., 2002; Siripurapu, V., et al., 2005; Vlahou, G. and F. Rivero, 2005). In contrast, no apparent DBC2 othrologs have been found in plants, fungi, bacteria and archea and are also absence from the model organisms *Caenorhabditis elegans, Xenopus laevis,* and *Saccharomyces cerevisiae* (Hamaguchi et al, 2002; Ramos, S., et al., 2002; Siripurapu, V., et al., 2005; Vlahou, G. and F. Rivero, 2005).

DBC2 has been shown to have numerous point mutations: Y284D, R275W, D299N, E349D, D368A, and F647T as well as several silent mutations and intron related point mutations (Knowles et al. 2005, Hamaguchi et al. 2002, Wilkins et al. 2004). In addition, two tumor specific mutations in the 5' UTR of DBC2 have been identified. One mutation possibly adds an additional transcription factor binding site, while the other eliminates two transcription factor binding sites including E2F1 (Ohadi et al. 2007). E2F1, which is known to regulate the expression of genes involved in cell cycle

progression and PCD, which has been shown to play a direct role in regulating DBC2 expression during the cell cycle (Freeman et al. 2007). Another study has indicated that the CpG islands within the promoter region of DBC2 are subject to aberrant methylation resulting in a significant decrease in DBC2 expression in cancerous tumors (Shi et al. 2008). Many of these mutations listed above do not show a definite phenotype and/or have not been tested for effects on currently known DBC2 protein-protein interactions.

However, the D299N and Y284D mutations in DBC2 have been shown to have a reduced ability to inhibit proliferation compared to wild type in a DBC2 null back ground (Hamaguchi et al. 2002, Wilkins et al. 2004). The D299N was identified in the initial screen of somatic missense mutations in breast tumor specimens (Hamaguchi et al., 2002). DBC2/D299N lacked anti-proliferation activity in T-47D (Human ductal breast epithelial tumor cell line) compared to wt DBC2, and this mutation was rescued by the reintroduction of the wild type protein (Hamaguchi et al., 2002)..

An additional investigation of other DBC2 mutants was conducted by Wilkins and co-workers (2004), who examined the capacity of the Y284D, D299N and D368A to interact with Cullin 3 (Cul3), the core component of Cullin-RING-Ligase (CRL) complexes, which functions as an ubiquitin E3 ligase. The binding of D299N and D368A to Cul3 was comparable to wt DBC2, whereas the Y284D failed to bind Cul3 (Wilkins et al., 2004). The binding interface of DBC2 for Cul3 was localized to the first BTB domain of the structure (Wilkins et al., 2004). Interestingly, the first BTB domain contains most of the currently identified DBC2 mutations (Knowles et al. 2005, Hamaguchi et al. 2002, Wilkins et al. 2004). This study further identified the functional interaction between DBC2 and Cul3 in regards to Cul3 activation. Cul3 is a protein that is regulated by neddylation. Neddylation is the covalent modification of an ubiquitin like modifier, nedd8, which causes a conformational change in the C-terminus of Cul3 that facilitates the transfer of ubiquitin onto the substrate (Choo et al, 2011). Neddylation of Cul3 stimulates the binding of the COP9 signalosome (CSN) to Cul3, which then catalyzes Cul3's deneddylation. CSN mediated deneddylation is essential

for Cul3 E3 ligase activity in vivo (Choo, et al 2001). DBC2 was shown to interact with both non-neddylated and neddylated Cul3, but not with any of the other cullin family members (Cul1,2,4a,5) (Wilkins et al. 2004). This study also demonstrated that DBC2 turnover resulted from Cul3 mediated ubiquitination of DBC2 and its degradation via the 26S proteasome, as DBC2 levels were increase over time upon treatment of cells with the proteaosome inhibitor MG132 (Wilkins et al. 2004).

Cul3 CRLs function in conjunction with a family of BTB-domain containing substrate receptors (Pintard et al., 2004). Wilkins and co-workers proposed a model in which DBC2 functions as an addition substrate receptor for Cul3 regulating substrate degradation via the Ubiquitin/26S proteasome pathway. Other BTB-containing substrate receptors have been shown to undergo auto-ubiquitination in a manner similar to that observed for DBC2 (Choo et al., 2011). The mutations in DBC2 that inhibit its Cul3 binding would result in the stabilization of both DBC2 and its substrate target proteins (Wilkins et al. 2004). It has recently been proposed that homo/heterodimerization between the Rho domain and BTB domain of the RhoBTB family members (see below) prevent DBC2 from forming a functional complex with Cul3, therefore stabilizing DBC2 and/or the other family members and preventing their degradation by CRL (Berthold et al. 2008). The Cul3 mutant study along with proteasome inhibition via MG132 is indicative of CRL being the complex that targets DBC2 for degradation. However, DBC2's role in targeting associated proteins for degradation similar to Actinfilin (a BTB-Kelch protein family member) targeting subunits of the GluR6 kainate receptor for degradation through Cul3 is premature (Salinas et al., 2006). Although both mutations have an effect that results in the loss of DBC2 anti-proliferation properties, D299N does not result in a loss of Cul3 binding as does the Y284D, indicating that DBC2 affects additional cellular pathways related to growth and differentiation (Wilkins et al. 2004).

Functional roles for DBC2 were investigated through microarray analysis using endogenous DBC2 expressed in HeLa cells. This study linked DBC2 to processes influencing apoptosis (Siripurapu et al., 2005). A recent study has linked the interaction of overexpressed DBC2 with Cul3 to increased apoptosis, possibly through DBC2 playing a role in Anoikis, as it reduces the ability of

cells to form anchorage independent colonies (Mao et al. 2011). The microarray analysis also linked DBC2 to pathways involved in cytoskeleton dynamics (McKinnon et al., 2008). DBC2's involvement in aspects of cytoskeleton dynamics is supported by its involvement in the regulation of the chemokine CXCL14 expression (McKinnon et al., 2008). CXCL14 is known to control cell migration and its expression is lost in a number of epithelial cancers (McKinnon et al. 2008). Another investigation linked DBC2 indirectly to cytoskeletal dynamics through the ability of ectopically expressed DBC2 to significantly increase levels of breast cancer metastatic suppressor (BRMS1), in conjunction with down-regulation of ezrin and Akt2 phosphorylation. Both BRSM1, and the Akt2/ezrin sytems affect the migration and invasion of cancer cells (Ling et al. 2010; Freeman et al. 2010). The additional pathways linked to DBC2 expression were membrane trafficking that was illustrated through DBC2-dependent microtubule-mediated transport of VSVG from the ER to the Golgi as well as the fluorescence localization of DBC2 to the microtubule network (Chang et al., 2006). Cell cycle progression which been illustrated by DBC2 modulated down regulation of cyclin D1 (Yoshihara et al 2007) and the E2F1 modulation of DBC2 expression described earlier with limited DBC2 localization seen in the nucleus (Siripurpa et al., 2005; Freedman et al., 2008; Yoshihara et al., 2007; Chang et al., 2006).

The DBC2 domain structure has undergone a limited amount of analysis in initial investigations (Figure 1, 4a & 8). The DBC2 Rho domain was determined to be deficient in binding GTP due to the inability of wt DBC2 and a truncated DBC2 (1-160AA) to bind GTP (Chang et al. 2004). However, the possibility that DBC2's GTP binding activity may be regulated through protein-protein interaction or post-translation modifications, as occurs in other G-protein, must be considered. In the classical small G protein system these assistance factors are(i.e guanine nucleotide exchange factor (GEF), GTPase activating protein (GAP), guanine nucleotide dissociation inhibitor (GDI) along with the newly coined GDI displacement factor (GDF) (DerMardirossian et al., 2005), but for DBC2 one must consider that it might also be an otherwise unknown functional partner. For example, GTP binding to DBC2 may require GEF catalyzed dissociation of tightly bound GDP for GTP

binding (figure 4) (Aspenstrom et al., 2004; 2007). The analysis was conducted via a Northwestern blot experiment with [α-^{32}P] GTP and *recombinant* DBC2 or truncated DBC2 (1-160AA) protein purified from *Escherichia coli* (Chang et al., 2006). It is plausible that wt DBC2 at 83 kDa had lost the ability to refold in an environment lacking molecular chaperones (e.g., DBC2 might require chaperones to prevent it from pursuing unproductive folding pathways, thus facilitating the folding process.) The question of proper folding is even more relevant to the truncated DBC2 (1-160AA), as sequence alignments demonstrated that truncating DBC2 GTP-binding domain back to a Ras rather than as a Rho domain, deleted a section of its GTP binding pocket and additional structure that undoubtedly stabilizes the domain fold.

A more comprehensive analysis of the amino acids must begin to determine the interactions of functional domains as single and/or complex entities. This will begin to elucidate the processes, which are hindered in the absence of DBC2.

Small G-proteins have highly conserved loop motifs required to bind and hydrolyze GTP (Paduch et al., 2001; Boureux et al., 2007). The loop motifs and overall structure currently accepted are derived from the ancestral small G-protein, Ras (Paduch et al., 2001; Boureux et al., 2007; Salas-Vidal et al., 2005). However, the Rho GTPase falls under the Ras superfamily that is sub-divided into 6 families: Ras, Rho, Rab, Ran, Arf and Micro. The Rho family is further subdivided into 8 subfamilies; Rho/Rif, Rac, RhoD, Cdc42, Rnd, RhoU/V, RhoH and RhoBTB (including DBC2) (Paduch et al., 2001; Boureux et al., 2007; Salas-Vidal et al., 2005). The Rho GTPase family has been shown to function in everything from cytoskeleton dynamics to programmed cell death (Knowles et al., 2005; Paduch et al., 2001; Salas-Vidal et al., 2005; Aspenstrom et al., 2004). Nonetheless, this well conserved family includes the atypical Rho GTPase subfamilies Rnd, RhoU/V, RhoH and RhoBTB (Aspenstrom, P., A., 2007). The sequence of the four subfamilies varies from that of the typical RhoGTPase (e.g., Ras) in conserved loop regions, catalytic residues (e.g. Ras conserved Gly 12 and Glu 61), absence of the characteristic isoprenyaltion CaaX motif, extended domain structure and/or regulation that is outside the control of the classical G-cycle (Figure 3). Each of the subfamilies

meets one or more of the listed criteria (Boureux et al., 2007; Salas-Vidal et al., 2005; Aspenstrom et al., 2007). Upon inspection of the DBC2 Rho domain, it was apparent that it had a domain structure containing amino acids that extended beyond the Ras domain structure.

The atypical small GTPase RhoH has been shown to be constitutively active, even with residue specific substitutions that render Ras defective in binding of GTP (Aspenstrom P., A., 2007). RhoH functions to inhibit pathways activated by typical Rho GTPases and has been shown to positively regulate the signal dependent activation of the protein kinase, Zap70. Thus, RhoH has been shown to maintain regulatory processes in both kinase and Rho dependent signaling (Aspenstrom P., A., 2007). Another atypical small GTPase, RhoU (Wrch-1) has been shown to have a rapid GDP $\Rightarrow$ GTP exchange, which produces a constitutively active form with no deleterious substitutions within the nucleotide bind region (Aspenstrom et al., 2004; Aspenstrom et al., 2007). The atypical subfamilies RhoH, RhoU/V, and Rnd have the ability to regulate the effectors (e.g. Pak1 & WASP) of G protein modifiers and the cycling proteins (e.g. RhoGDI) required for typical and atypical Rho GTPase activity (Aspenstrom et al., 2007; Masuda-Robens et al., 2003). The influence of guanine nucleotide binding on function of the RhoBTB subfamily is still to be investigated. The appropriate sequence motifs to be classified as a Rho GTPase are not present within the provisional Rho domain of RhoBTB3, thus it is excluded from many analyses of this atypical subfamily; even though it is the only

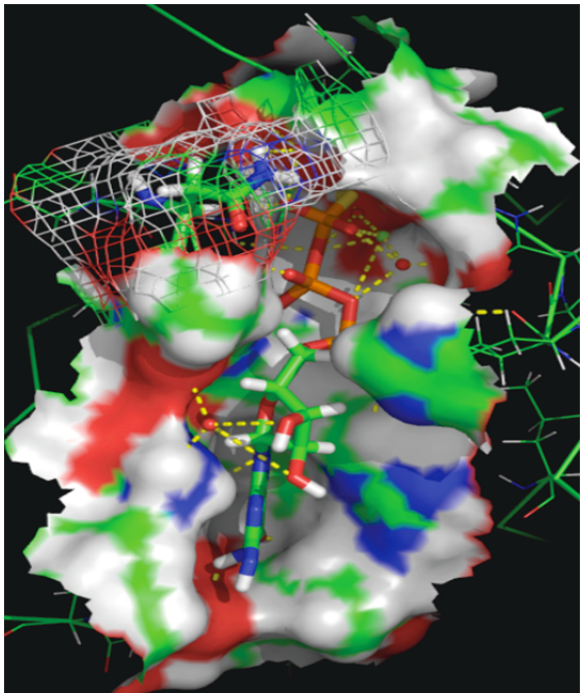

Figure 2: Ligand site of DBC2 Rho domain in complex with GTγS (sticks), Asn 23 mesh. Residues colored by element CHNOSP, Mg ion green sphere, water red sphere and the yellow dashed lines indicate polar contacts. GTγS docking completed by Sybyl `version 7.0, Tripos and rendered in` PyMOL, Delano Scientific. Sybyl docking was completed by Donna J. Lubbers, University of Kanas.

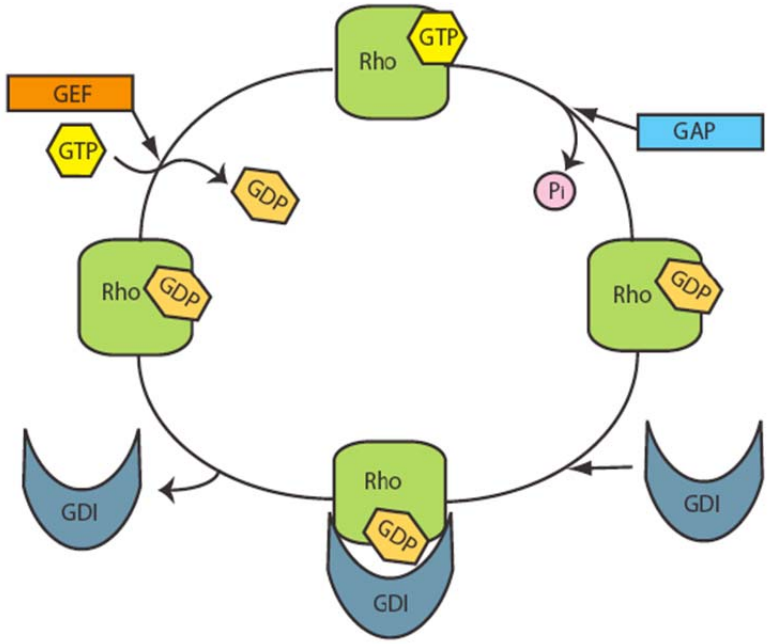

Figure 3: Classical regulatory small G protein cycle (G-cycle). Cyclic protein include the GEF, GAP, GDI, GDP, GTP and P_i, colored orange, blue, gray, tan, yellow and mauve, respectively.

member to retain the isoprenylation motif at its C-terminus (Boureux et al., 2007; Salas-Vidal et al., 2005; Aspenstrom et al., 2007). The RhoBTB1 and RhoBTB2 (DBC2) sequences lack the conserved Q (Ras position Q61) that is necessary for catalysis of GTP hydrolysis in classical Rho GTPases (Chang et al., 2004; Paduch et al., 2001; Boureux et al., 2007; Salas-Vidal et al., 2005). DBC2 also contains substitutions for classical consensus residues at G⇒N in the P-loop, A ⇒ F in switch I, a (T/N) ⇒ C of loop G4 and A ⇒ V of loop G5 (Table 1) (Paduch et al., 2001; Boureux et al., 2007). The alterative residues located in the classically conserved binding/catalysis regions of the DBC2 Rho domain is suggestive of a function similar to the other atypical Rho GTPases, which remain in a constitutively GTP bound state (Berthold et al., 2008; Aspenstrom et al., 2007).. Shown in more comprehensive sequence alignment is the reoccurrence of the consensus (T/N) ⇒ C substitutions that occurs in loop G4, which many Rho and Rnd proteins also contain (Boureux et al., 2007; Salas-Vidal et al., 2005; Aspenstrom et al., 2007). The alteration of the classical consensus sequences of this atypical family could yield the regulatory functions necessary for their tissue specificity (Knowles et al., 2005; Ramos et al., 2002; Cho et al., 2007; Aspenstrom et al., 2007; Bement et al., 2006; DerMardirossian et al., 2005; Chen et al., 2006; St-Pierre et al., 2004). The exclusive nature of this family is debatable with the identification of RhoBTB family members in many immortalized cell lines currently in laboratory use.

The substitutions deviating from consensus for the DBC2 Rho domain were reported by Chang, F.K et al. (2006), to interrupt the ability of DBC2 to bind GTP. However, the Ras domain (e.g., only the first 160 AA) was used to evaluate the GTP binding capacity of the DBC2 (Chang, F.K., et al., 2006). For the Rho structure this would result in a loss of loop G5, which has been determined to decrease affinity and hinder base discrimination (Paduch, M.F., et al., 2001). The substitution of G ⇒ N in the P-loop (Ras positionGly12) puts the Asn in a curious position directly over the predicted binding pocket of the GTP γ-phosphate (Figure 2). This could result in a novel form of self-regulation that engages other domains/motifs within the DBC2 architecture resulting in a

constitutively active and/or rapid cycling form, that were mentioned previously (Paduch, M.F., et al., 2001). There is a precedent for Asn to have the capacity to be involved in GTP hydrolysis without the presence of the catalytic Q61 (Ras reference). For example, Rap1Gap utilizes an Asn rather than an Arg finger to catalyze the GTP hydrolysis. Rap1 harbors a substitution of the catalytic conserved Q which is replaced by a Thr (Table 1) (Daumke et al., 2004; Rehmann et al., 2004). While the mechanism of GTP hydrolysis was not fully elucidated, site-directed mutagenesis of the Asn indicated that it was essential for Rapl GTP hydrolysis, with its motif being referred to as the Asn thumb (Daumke et al., 2004; Rehmann et al., 2004). This proposes that hydrolysis of GTP can occur without the presence of the conserved Q61 that is retained by most classical small G proteins (Daumke et al., 2004; Rehmann et al., 2004). Another example is the Ran GTPase shown to use a Tyr to activate the Glu for catalysis without donated residues from the RanGap (Seewald et al., 2002). The RanGAP instead acts in reorienting the native Ran residues into the correct orientation for efficient hydrolysis (Rehmann et al., 2004, Seewald et al., 2002). Another alternative to classic GAP hydrolysis is the TBC domain that facilitates the hydrolysis of GTP bound Rab, through a dual finger mechanism donating both the Arg and Glu necessary for catalysis (Pan et al., 2006). The classical Arg finger, as well as the other alternatives have a possibility to facilitate hydrolysis of GTP bound DBC2. However, DBC2's native residues are conceivably able to neutralize the charge of the bound GTP molecule (Paduch et al., 2001; Daumke et al., 2004; Rehmann et al., 2004; Seewald et al., 2002; Pan et al., 2006).

The mechanisms for nucleotide binding must be re-investigated to elucidate how the DBC2 Rho domain is regulated. This includes any accessory proteins, post-translational modifications and/or, cofactors influencing the regulatory control for GTP binding.

The tandem BTB domains that follow the Rho domain are the next functional domains (Figure 1). The mutations known to affect DBC2 function have been predominately localized to the first BTB domain (figure 1). Three of these mutations have been examined with moderate overall analysis as previously described (Hamaguchi et al., 2002; Freeman et al., 2008; Wilkins et al., 2004).

The general structure and functional properties attributed to the BTB protein families have been elucidated. BTB-domain containing proteins participate in many cellular and physiological functions, including: transcriptional regulation and chromatin remodeling; response to DNA damage; regulation of the cell cycle; cytoskeleton dynamics; embryonic development; cell differentiation; regulation of ion channels; protein degradation; and tumorigenesis (Hori et al., 1999; Kelly et al., 2006; McEvoy et al., 2007; Perez-Torrado et al., 2006; Pintard et al., 2004; Stead et al., 2007; Stogios et al., 2005; Vadlamudi et al., 2003; Welcker et al., 2003; Wimuttisuk et al., 2007). The BTB/POZ domain families contain the BTB structural core fold, which is the major protein recognition motif, with a β1/β2/α1/α2/β3/α3/α4/α5 (β = β sheet), (α = α helix) topology, while the amino acid

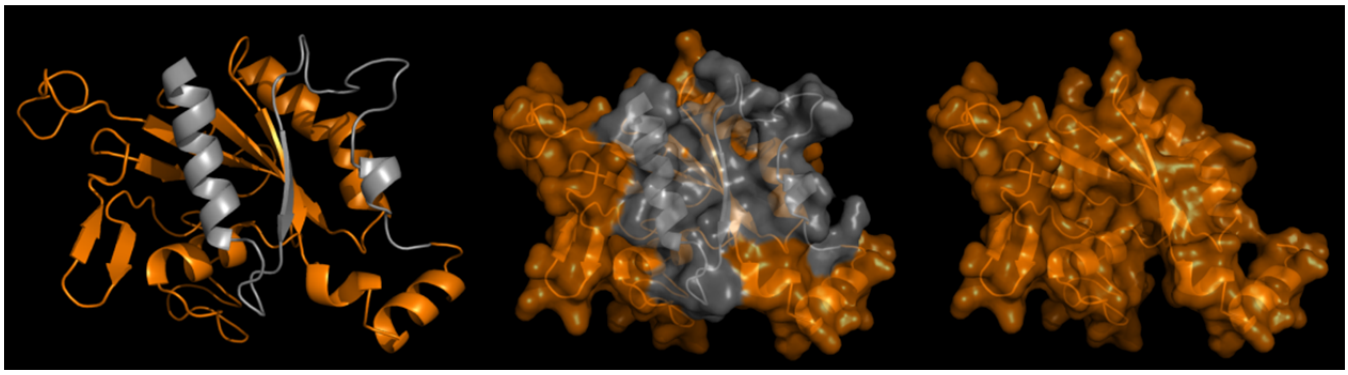

Figure 4: DBC2 Rho domain homology model amino acids 1-206. Gray indicates missing residues due to dissection at amino acid 160 (Right) Cartoon display DBC2 Rho domain. (Middle) Transparent surface DBC2 Rho domain (Left) Transparent surface DBC2 Rho domain dissected at amino acid 160. Rendered by PyMOL, Delano Scientific

Protein	Sequence	G1(P-loop)	G2(switch I)	G3(switch II)	G4	G5
RhoBTB1	O94844	GDNAVGKT	PTV	DTFG- -	CQLD	TSV
RhoBTB2	Q9BYZ6	GDNAVGKT	PTV	DTFG- -	CQLD	TSV
DBC2 (RhoBTB2)	P63000	GDGAVGKT	PTV	DTAGQE	TKLD	CSA
Cdc42	P60953	GDGAVGKT	PTV	DTAGQE	TQID	CSA
RhoA	P61585	GDGACGKT	PTV	DTAGQE	NKKD	CSA
Rap1A	P62834	GSGGVGKS	PTI	DTAGTE	NKCD	SSA
H-Ras	P01112	GAGGVGKS	PTI	DTAGQE	NKCD	TSA
Ran	P62826	GDGGTGKT	ATL	DTAGQE	NKVD	FVA
Consensus		(GXXXXGKT)	(XTX)	(DXXG)	(N/T)(K/Q)XD	(T/G/C)(C/S)A

Table 1: Alignment of small G-protein conserved loops, G1-G5 are involved in binding GTP. Complete conserved residues in yellow, G1-G5 loop consensus sequences in parenthesis. Sequence accession are listed, source SWISSPROT. The previous study of DBC2 GTP binding capabilities (Chang, F.K, et al., 2006), is missing the C-terminal 45 amino acids including the G5 loop of the DBC2 Rho domain

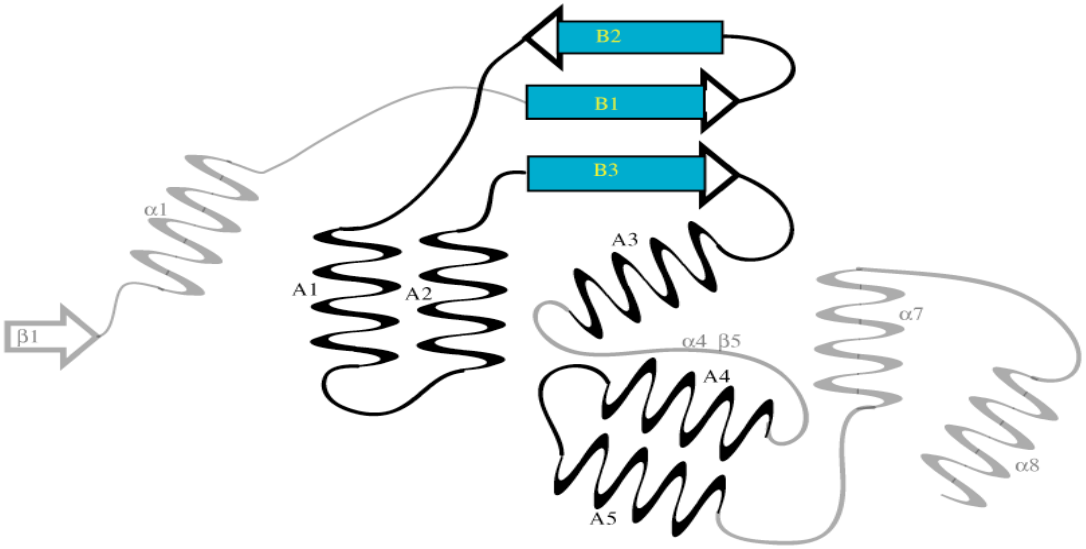

Figure 5: BTB family domain organization. The black helices (A1/A2/A3/A4/A5) and blue sheets (B1/B2/B3) form the BTB core. The extensions (β1/α1, α7/α8) and internal (α4/β5) structural elements specific to subfamilies are in gray. The loop between A3 and A4 is gray due to its variable length with a tendency to contain subfamily specific elements. Adapted from Stogios et al, 2005

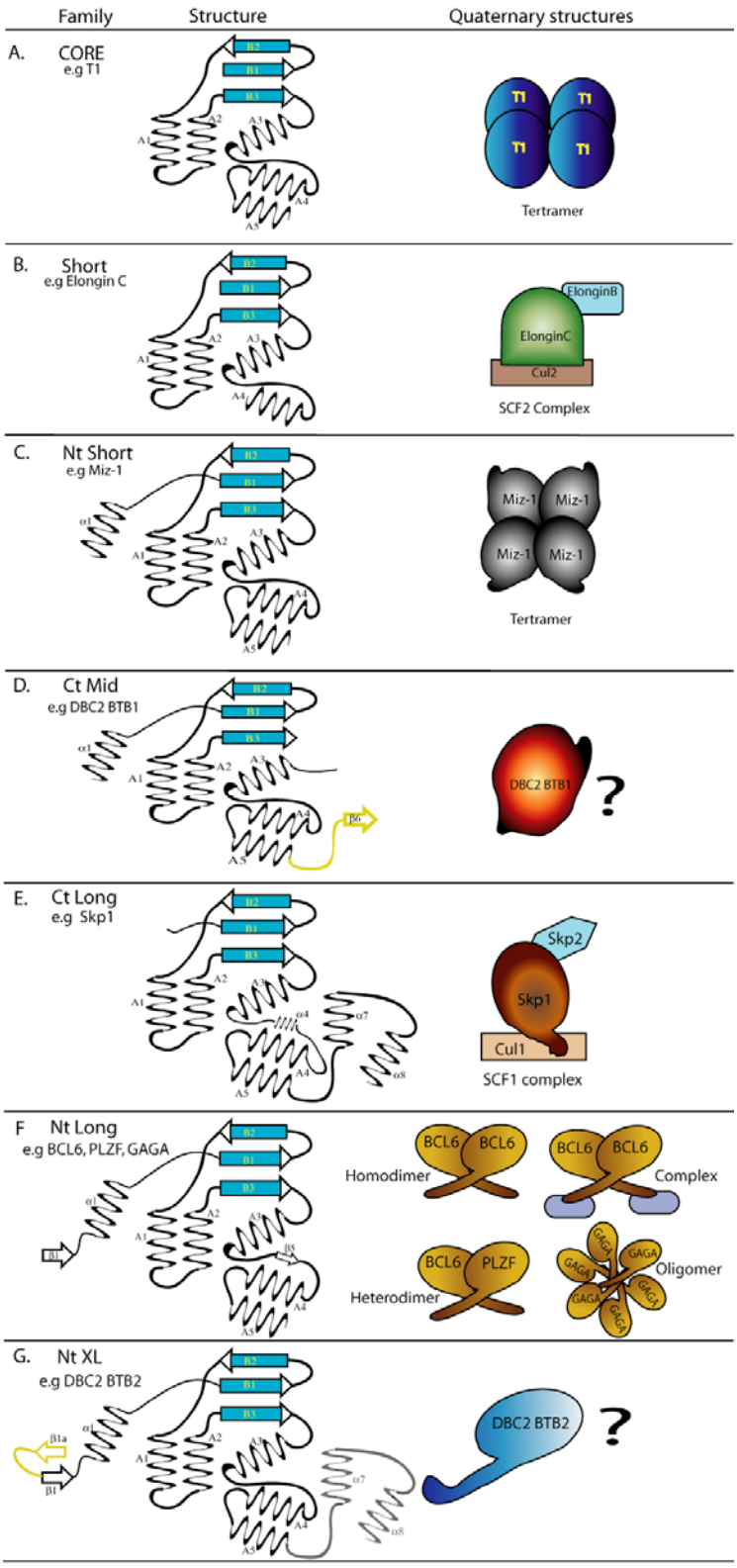

Figure 6: BTB family quaternary structures formed by the various tertiary domain arrangements.

sequences of BTB domains showing very limited similarity (figure 5 & 6) (Kelly et al., 2006; Perez-Torrado et al., 2006; Pintard et al., 2004; Stead et al., 2007; Stogios et al., 2005). The sequence conservation is concentrated to residues in the hydrophobic core of the fold, predominately located in the β1, α3 and α4 of the core structure (figure 5 & 6) (Stogios et al., 2005). The core is either N-terminal, C-terminal or internally extended as the structures of the BTB subfamilies diverge (Figure 5 & 6) (Stogios et al., 2005). T1 (core) is composed of only the BTB core, while PLZF/BCL6 (Nt-long) have a N-terminal β1/α1 and β5 specific elements, with Skp1 (Ct-long) adding an α4 and C-terminal α7/α8; ElonginC (short) lacks the A5 of the BTB core structure (figure 5 & 6) (Stogios et al., 2005). An additional BTB fold has been illustrated in the Miz-1 (Nt-short) structure containing a N-terminal α1 in addition to the core fold without the β1 indicated for Nt-long form (Figure 5 & 6) (Stead et al., 2007).

Taking these features into consideration the BTB structural elements residing distal and proximal to the essential core are variable outside of the current structural families. However, the organization of the BTB domain confers its functional topology with most functioning as dimers, with many forming higher order structures such as tetramers and oligomers (figure 6) (Kelly et al., 2006; Perez-Torrado et al., 2006; Pintard et al., 2004; Stead et al., 2007; Stogios et al., 2005). The oligomerization state of proteins depends on the structural elements within each individual BTB domain (Figure 6) Kelly et al., 2006; Perez-Torrado et al., 2006; Stead et al., 2007; Stogios et al., 2005; van den Heuvel et al., 2004). The additional domains associated with a BTB domain results in their segregation into families. The MATH (Meprin and TRAF Homolog)-BTB, BTBk (BACK-Kelch), Rho-BTB, T1, Skp1, ElonginC and BTB-ZF (zinc finger) are the current conserved BTB protein families (Kelly et al., 2006; Perez-Torrado et al., 2006; Pintard et al., 2004; Stead et al., 2007; Stogios et al., 2005). The MATH-BTB is the most common BTB domain containing family (Kelly et al., 2006; Perez-Torrado et al., 2006; Pintard et al., 2004; Stead et al., 2007; Stogios et al., 2005). BTB domains are generally positioned at the N-terminus of the domain arrangement (Kelly et al.,

2006; Perez-Torrado et al., 2006; Pintard et al., 2004; Stead et al., 2007; Stogios et al., 2005). The BTB proteins have a plant-specific family, BTB-NHP_3, which is thought to be an adaptor for a light activated signaling pathway (Stogios et al., 2005). Conversely, no BTB containing proteins have been identified in bacteria or Archaea (Stogios et al., 2005). The arrangement of the BTB domains of DBC2 is an atypical arrangement with the BTB domains flanked at the N-terminus and C-terminus by an atypical Rho GTPase and a putative RING domain (figure 1). The domain arrangement of DBC2 comprised of two BTB domains postulates a potential lack of hetero or homo-quaternary forms for functionality. Due to this, DBC2 has a deficiency in exclusive classification and adherence to consensus parameters. This exemplifies the perception that DBC2 is an atypical protein, which potentially deviates from the functional activities known to the domains represented in the DBC2 architecture.

BTB protein families are quite diverse in structure and function, however; many share a common theme, substrate degradation via the ubiquitin/26s proteasome (figure 7). The pathway for protein ubiquitinylation/degradation involves three enzymes the E1 (Ubiquitin-activating enzyme), the E2 (Ub-conjugating enzyme) and the E3 (Ubiquitin -ligating enzyme a.k.a Ub-ligase) (Knowles et al., 2004; Siripurapu et al., 2005; Hori et al., 1999; McEvoy et al., 2007; Pintard et al., 2004; Vadlamudi et al., 2003; Welcker et al., 2003; Wimuttisuk et al., 2007). The E1 activates the ubiquitin molecules with ATP followed by the covalently binding of ubiquitin to the E1 upon formation of a thiol-ester bound. The E1-bound ubiquitin is then transferred to the E2 through the formation of a thioester bond. The E2 subsequently: 1) transfers the ubiquitin to a E3(HECT) target complex for subsequent HECT catalyzed transfer of ubiquitin to the substrate; or 2) associates with an E3 (RING) complex, which ubiquitinates substrates by direct transfer of the ubiquitin from the E2 to the E3 complex bound substrate (Pintard et al., 2004). The C-terminal glycine of ubiquitin is used to form an isopeptide bond with the epsilon

amino group of Lys residues. The ubiquitin can then be extended and have been shown to be arranged into chains by attaching to lysine 6, 11, 27, 29, 33, 48 or 63 of other ubiquitin molecules before or after initial target protein attachment (Pintard et al., 2004).

In this scheme, BTB proteins are shown to be an integral component of the Cul3 RING-H2-type E3 ligase complex; CRL (Hamaguchi et al., 2002; Hori et al., 1999; McEvoy et al., 2007; Pintard et al., 2004; Vadlamudi et al., 2003; Welcker et al., 2003; Wimuttisuk et al., 2007; Singer et al., 1999). There are a number of the additional physiological responses associated to the BTB proteins, but protein degradation has been shown to be a common link to most of the BTB families. The Skp1/Cul1/Rbx/F-Box, SCF1, is potentially the most notable substrate degradation complex involving a BTB protein to date. But has been expanded to incorporate ElonginC/Cul2/ElonginD/SOCS, and Cul3/BTB/Rbx, CRL (Hori et al., 1999; McEvoy et al., 2007; Pintard et al., 2004; Vadlamudi et al., 2003; Welcker et al., 2003; Wimuttisuk et al., 2007; Singer et al., 1999).. Ligase complexes all function in the ubiquitinylation of proteins signaled for degradation

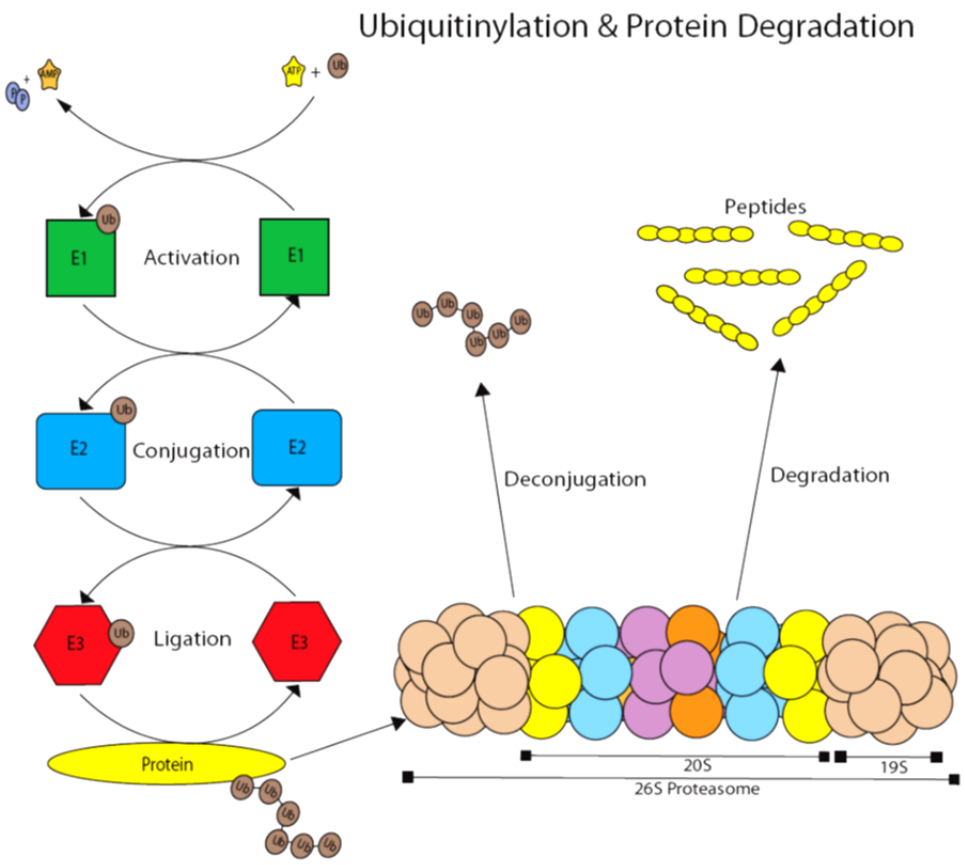

Figure 7: Ubiquitin/26S Proteasome scheme. Adapted from Boston Biochem (www.bostonbiochem.com)

(Hamaguchi et al., 2002; Hori et al., 1999; McEvoy et al., 2007; Pintard et al., 2004; Vadlamudi et al., 2003; Welcker et al., 2003; Wimuttisuk et al., 2007; Singer et al., 1999). The DBC2 interaction gaining the most momentum is the DBC2 Cul3 complex, previously mentioned (Wilkins et al., 2006). The evidence that Cul3 binds DBC2 is adequate (Arnold et al., 2006; Kopp et al., 2006; Blom et al., 2004; Kopp et al., 2006; Schwede et al., 2004; Bennett-Lovsey et al., 2008), but the conclusion that the second BTB domain's lack of interaction with Cul3 is debatable (figure 8b). The deletions made by Wilkins et al (2004), are consistent for the Rho and bipartite BTB domain. However, upon further analysis, the second BTB domain extends further upstream then the dissection point that was used (figure 8a) (Arnold et al., 2006; Kopp et al., 2006; Blom et al., 2004; Kopp et al., 2006; Schwede et al., 2004; Bennett-Lovsey et al., 2008). As predictions for BTB domains were made using only the BTB core and not the N-terminal and C-terminal extensions specific to families (Stogios et al., 2005; Finn et al., 2006). The interaction of the second BTB domain with Cul3 or additional cullins raises to possibility that DBC2 can form multiple degradation complexes as suggested by Perez-Torrado et al. 2006. Therefore, the overall regulation of signaling motifs, modifications and the tentative RING domain must be examined, to gain insight into how specific domains function to: 1) regulate intramolecule interactions within DBC2 and interactions of DBC2 with other protein: 2)modulate DBC2's localization, as its contains a nuclear localization sequence and likely undergoes nuclear/cytoplasmic shuttling; and/or 3) determine the physiological significance DBC2 in normal cellular dynamics, as well as tumor progression or impedance.

A.

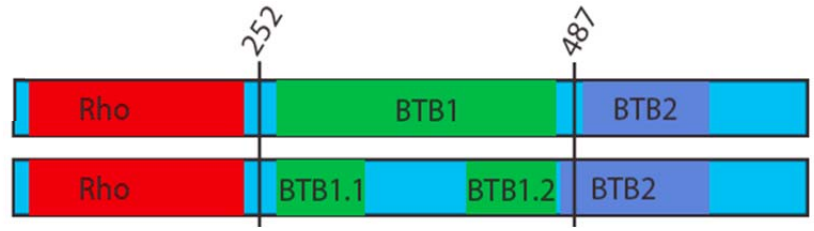

B.

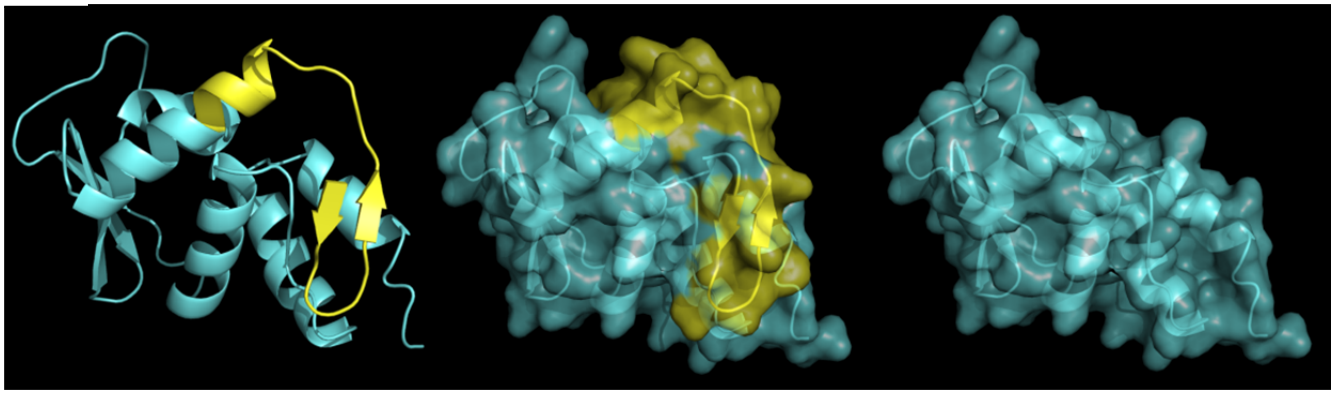

Figure 8: A.) Top DBC2 domain arrangement from Wilkins et al, 2006. Bottom current depicted DBC2 domain arrangement, dissection points indicated by vertical line with amino acid number. B.) PHYRE predicted homology model of the DBC2 BTB2 domain. (Right) Cartoon display with the yellow indicating missing residues (amino acids 466-486) (figure 8a) (middle) Transparent surface display (left) Transparent surface without missing residues. The putative C-terminal extension omitted for clarity. Rendered by PyMOL, Delano Scientific

A comprehensive analysis of DBC2 must consider the known DBC2 mutants that create impairments or enhancements, and is assessed here in order of increasing AA residues, as in Figure 1 (Knowles et al. 2005, Hamaguchi et al. 2002, Wilkins et al. 2004); Chang et al., 2006). The V245A mutation lies inside the Pro-rich region, but is a residue of the predicted PEST motif. The online program PEST finder (Rechsteiner et al., 1996; Rogers et al., 1986) predicts that the V245A mutation (Stogios et al., 2005; Finn et al., 2006) increase the probability that the region functions as PEST motif, thus raising the possibility that the mutation shortens the half-life of the protein and decreases its availability. The next mutation is the R275W, which has the potential of disrupting the conserved core fold R275 is predicted to be a solvent exposed residue of the β2 strand (unpublished data).

Next, the Y284D mutation results in hindered binding of Cul3 leading to an extended DBC2 lifetime (Wilkins et al., 2006). However, the Y284D mutant would be incapable of targeting substrates to Cul3 for ubiquitination, and thus not be able to carry out its normal cellular function.

The effect of the D299N mutation on DBC2 function was the first to be investigated in T47-D cells by Hamaguchi et al (2002). The mutation impeded and/or abolished the anti-proliferation effects of DBC2 compared to wild-type DBC2. Upon further analysis, the mutation results in the loss of a clathrin box motif that is present on cargo adaptor proteins (Puntervoll et al., 2003; MotifScan). This alteration has the potential alter a regulatory motif that may function in vesicular trafficking reported by Chang et al (2006).

The next mutant, D368A is predicted to result in the loss of a PDZ binding motif and a CKII (casein kinase 2) phosphorylation motif (Puntervoll et al., 2003; MotifScan). The three mutants D299N, D368A and E349D (which shows no apparent motif alterations) are all located in the bipartite linker region that has a substantial probability to participate in the regulation of the first BTB domain and/or the overall DBC2 structure. The analysis of this region predicts a number of possible regulatory motifs, all having the capability to contribute to DBC2 regulation (Blom et al., 2004; Rechsteiner et al., 1996; Rogers et al., 1986; Puntervoll et al., 2003; MotifScan).

The G561S mutant is predicted to gain four motifs: a CK I (casein kinase 1), GSK3 (Glycogen synthase kinase 3), SRC kinase and p38MAPK (p38 Mitogen-activated protein kinase phosphorylation site (Blom et al., 2004; Puntervoll et al., 2003; MotifScan) This mutation is located in the turn leading from the α3 to the α4 core helix. This substitution could affect the stability of the helix with the possibility of further disruption, if the residue is targeted for phosphorylation.

The final known mutation is, F647T that is predicted to cause multiple possible alterations in function. This mutation is positioned within the putative RING domain (unpublished data). The putative RING domain is based on NBCI PSI-BLAST analysis related to NOT4, which consequently has been shown to have E3 ligase activity (Albert et al., 2002; Hanzawa et al., 2001). This substitution located two residues C-terminal of the final Cys has the potential to disrupt the putative $C_2H_2C_2$ motif. The motif of this putative RING domain differs from NOT4, C_4C_4, and shows a relative similarity to the Hrt1, $C_3H_2C_2$, which also has E3 ligase activity (Hanzawa et al., 2011; Mulder et al., 2007; Seol et al., 1999). The predicted motifs created by this mutation have the potential to be destabilizing. The mutation also creates a p38MAPK, cdk5, (cyclin-dependent kinase 5), CKII, PKC, (protein kinase C), and a ProD-kin1, (proline-directed kinase 1), phosphorylation motifs, and it also creates predicted FHA (Forkhead associating) and WW binding motifs that could generate multiple new regulatory signals (Blom et al., 2004; Puntervoll et al., 2003; MotifScan).

In conclusion, DBC2 is a newly identified tumor suppressor which has not be subjected to extensive analysis. Its functional nature is still quite a mystery whereas the deciphering of the addition or loss of multiple motifs associate with inborn mutation along with protein-protein interactions, regulatory effects and localization of responses would be valuable in understanding the cellular pathways manipulated in response to DBC2. The identification of protein-protein interactions will aid in identifying initial functional and physiological responses to be investigated as they relate to DBC2. Studies have been conducted identifying some physiological response to the presence or absence of DBC2, but have overlooked the functional regulation of DBC2 itself and the additional complexes that form to orchestrate these responses. The curious domain structure of DBC2 requires

that a wide variety of regulatory mechanisms to be explored. While, DBC2 has been identified as a tumor suppressor protein only a marginal amount of investigations have looked into the mechanism of action related to this function. The focus of the next chapter is on the characterization of DBC's GTP, binding activity, and its interactions with other proteins.

CHAPTER II

Functional Modulation of DBC2 by the Molecular Chaperone Hsp90

Introduction

It is estimated that approximately 290,000 new breast cancer cases will be diagnosed in the United States alone for 2011 (Breast cancer facts & figures 2011-2012). They will be joining the estimated 2.6 million U. S. women who are already living with a history of breast cancer. Inherited mutations account for approximately 5-10% of breast cancer cases, with mutations in the BRAC1 and BRAC2 genes only accounting for less than a quarter of the familial cases (Breast cancer facts & figures 2011-2012). An additional contributing gene, Deleted-in-Breast Cancer 2 (DBC2, a.k.a RhoBTB2) was identified in a region of human chromosome 8p21, which was found to be homologously deleted in 3.5% of breast tumors (Hamaguchi et al., 2002; Mao et al., 2011). In addition, expression of DBC2 was found to be silenced in 42% of breast cancer cells or tissues (Hamaguchi et al., 2002). Subsequent studies found that DBC2 expression was suppressed in approximately 60% of breast cancers (Mao et al., 2010), 50% of lung cancers (Wilkins et al., 2004), and 75% of bladder cancers (Shi et al., 2008). Loss of DBC2 expression in bladder cancer was found to be associated with hypermethylation of the gene's promoter (Shi et al., 2008). Furthermore, missense mutations in the DBC2 gene were also identified (Hamaguchi et al., 2002, others). Ectopic expression of wild-type DBC2, but not its mutants, in T-47D

breast cancer cells lacking DBC2 expression caused growth inhibition (Hamaguchi et al., 2002).

While DBC2 is now firmly established to be an important tumor suppressor gene, little is known yet about its physiological function. DBC2 is an atypical protein containing an amino-terminal Rho domain followed by a proline-rich region, two tandem BTB domains and a conserved C-terminal domain with unknown function. The BTB domain is so named as it was originally found in Drosophila transcription factors *Bric à Brac, Tramtrack*, and *Broad Complex* (Dhordain et al., 1995). Besides transcription, BTB-containing proteins are involved in a wide range of biological processes, including the cell cycle and apoptosis (Berthold et al., 2008).

Microarray analysis indicated that DBC2 modulates the expression of gene networks that regulate cell growth via cell cycle control and apoptosis, and that are related to cytoskeletal and membrane trafficking (Siripurapu et al, 2005). DBC2's ability to suppress cell growth has been biochemically linked to its ability to down-regulate cyclin D1 expression (Yoshihara et al., 2007). In addition, the DBC2 gene has been shown to be a direct target of the E2F1 transcription factor, whose primary function is to modulate the expression of genes involved in cell cycle progression and apoptosis (Freeman et al., 2007). DBC2 expression has also been demonstrated to be required for the expression of the chemokine, CXCL14 (McKinnon et al., 2008). While CXCL14 is expressed in most normal cells, its expression is very low or absent in many cancerous cells and tumors (Shellenberger et al., 2004), particularly those of epithelial cell origin.

DBC2 's association with the cytoskeleton and membrane trafficking is supported by the observation that DBC2 functions to facilitate microtubule-mediated transport of vesicular stomatitis virus glycoprotein (VSVG) from the endoplasmic reticulum (ER) to the Golgi apparatus (Chang et al., 2006). Furthermore, inhibition of the migration and invasion abilities of MDA-MB-231 and MDA-MB-435 metastatic breast cancer cell lines upon ectopic overexpression of DBC2 was associated with increased expression of breast cancer metastasis

suppressor BRMS1 and decreased phosphorylation of ezrin, a key signaling molecule that regulates cell migration and invasion (Chang et al., 2006; Ling et al., 2010).

The BTB-domain has structural homology with Skp1, a component of Cullin1 ubiquitin ligase complex and directs the docking of a subset of BTB-proteins to Cullin3 (Cul3). The Cul3-bound BTB-domain containing protein functions as a substrate specific adapter for Cul3 ubiquitin ligase complexes (Willems et al. 2004). DBC2 has been demonstrated to interact directly with Cul3, and its levels appear to be auto-regulated through its interaction with the Cullin3 (Cul3) ubiquitin ligase complex (Freeman et. al., 2007; Wilkins et al., 2004.). Tumor cell resistance to the overexpression of DBC2 is mediated via DBC2's rapid destruction by the 26S proteasome (Collado et al. 2007).

All the functions listed above have been proposed to occur without the binding of the Rho domain to GTP (Chang et al., 2006). In this study, we show that DBC2 is a substrate (client) protein of the Hsp90 chaperone machine. In addition, DBC2 was found to have retained the capacity to bind GTP like the atypical Rho GTPases Rnd and RhoH. Furthermore, DBC2's GTP binding ability was modulated by the Hsp90 chaperone machine with the inhibition of Hsp90 ATPase cycle resulting in decreased or increased GTP binding, which correlated with inhibition of Hsp90's entry or exit from its ATPase cycle, respectively. Hsp90 is also demonstrated to modulate the association of DBC2 with components of Cul3 ubiquitin ligase complexes.

Experimental Procedures

Deletion Constructs:

All deletion mutants were constructed with the pcDNA3.1 vector. All N-terminal deletion constructs containing truncations of the DBC2 ORF corresponding to specific structural regions, contain a *pfu* PCR derived Flag epitope tag at the 5' end of the amplified insert. C-terminal deletions of specific structural regions were constructed using site-directed mutagenesis (Stratagene) to insert stop codons at desired locations using the full-length pcDNA3.1 Flag-DBC2 as a template.

In vitro coupled transcription/translation (TnT):

Flag-tagged DBC2 and each deletion construct was synthesized by couple transcription/ translation (TnT) in nuclease-treated rabbit reticulocyte lysate (RRL) (Craig et al., 1992) containing [^{35}S]-methionine for 30 min at 30°C in the presence or absence of 10 μg/mL geldanamycin, DMSO, 20 mM sodium molybdate (MoO4), or deionized water. Where noted, Flag-DBC2 or deletion constructs were synthesized by TnT (T7 PCR TnT® Quick Master mix, Promega) supplemented with either [^{35}S]-methionine or non-radioactive methionine for 90 min at 30°C in the presence or absence of 10 μg/mL GA, DMSO, 20 mM sodium molybdate (MoO4), or deionized water For the TnT of Flag-DBC2 and its R99G, and V191I mutants, each construct was synthesized by PCR using the *pfu* polymerase (Aligent) with PCR primers containing a T7 promoter and poly-A extensions at the 5' and 3' end, respetively according to manufactures protocol. The amplified DNA was then added to the TnT (Promega) supplemented with [^{35}S]-methionine for 90 min at 30°C in the presence or absence of 10 μg/mL GA, DMSO, 20 mM sodium molybdate (MoO4), or deionized water. In all cases, naïve RRL containing no template DNA was used as the control for the nonspecific binding.

Immunoprecipitation/GMP/GTP/Neutravidin/UBE pull-down assay:

All samples were placed on ice, and then clarified by centrifugation for 7 min at (16,000 x g) prior to the immuno-adsorptions or pull downs. Samples were added to 12.5 µl IgG resin containing pre-conjugated anti-Flag-tag IgG (Sigma), 25 µl of GMP- or GTP-agarose, or 20 µl of Neutravidin- or UBE-linked agarose. Samples were incubated with resin for 1 hr at 4°C with mixing. Samples were then washed four times with either low salt buffer containing, 10 mM Pipes (pH 7.4), 100 mM NaCl, and 0.5% Tween 20 (P100T) or once with P100T, twice with high salt buffer containing 500 mM NaCl (P500T), followed by a wash with P100T. Samples were boiled in SDS sample buffer, and analyzed by SDS-PAGE on an 8% gel, followed by electrotransfer to PVDF membrane (BioRad), followed by autoradiography or Western blotting for co-adsorbed proteins. Samples quantified by scintillation counting were added to scintillation cocktail immediately following the final wash step and counted. Samples for mass spectrometry were eluded from the Flag immunoresin by 100 mM ABC, 8 M urea and 4 mM EDTA. Elution was carried out at 4°C for 30 min, and then supernatant was removed and stored at -80°C until LC-MS/MS analysis with an Obitrap XL mass spectrometer.

Mammalian Whole Cell lysate preparation:

MCF-7 and/or HeLa cells were grown to confluence in either 75 cm^2 or 150 cm^2 flasks in DMEM medium at 37 °C in 5% CO_2. Cells were detached using 0.25% trypsin for 10 min at 37°C. Cells were then pelleted and washed once in fresh DMEM medium. Following two additional washes in ice cold mammalian wash buffer, containing 35 mM Hepes pH 7.5, 140 mM NaCl and 11 mM glucose, the cells were mixed 1:2 in mammalian cell lysis buffer, containing 20 mM Hepes pH 7.7, 140 mM KOAc, 1.0 mM $Mg(OAc)_2$. The suspension was then placed into a Parr nitrogen disruption chamber (Parr Instrument Company.) The Parr chamber was equilibrated with

nitrogen to 1200-1500 psi for 30 min at 4^0C with stirring of the cell suspension during the equilibration. After equilibration, the pressure was released and the lysate collected. After collection, the lysate was centrifuged at (16,000 x g) for 12.5 min at 4°C. Following centrifugation aliquots of lysate made, snap frozen in liquid N_2 and stored at 80°C until use.

Immunoprecipitation of DBC2 complexes reconstituted with HeLa or MCF-7 whole cell lysate for analysis by LC-MS/MS.

At the completion of Flag-tagged DBC2 synthesis by TnT, samples (200 µl) were mixed with 50 µl of either HeLa or MCF-7 whole cell lysate (WCL) prepared as described above, followed by incubation for 20 min at 30 ^{o}C.. The samples were then placed on ice, and clarified by centrifugation for 12.5 min at (16,000 x g) prior to the immuno-adsorptions. Samples were added to 30 µl anti-flag agarose (Sigma), incubated with resin for 1 hr at 4°C with rocking, and then washed five times with buffer containing, 10 mM Pipes (pH 7.4), 150 mM NaCl, (P150). Proteins were eluted from the anti-Flag agarose with 100 mM ABC, 8 M urea and 4 mM EDTA. Elution was carried out at 4°C for 30 min. The supernatant was removed and stored at -80°C until LC-MS/MS analysis with an Obitrap XL mass spectrometer or the eluted samples were boiled in SDS sample buffer, and analyzed by 8% SDS-PAGE followed by electrotransfer to PVDF membrane (BioRad) for Western blotting for co-adsorbed proteins.

The LC-MS/MS analysis of DBC2 associated proteins:

The LC-MS/MS data was compiled by Scaffold for protein identification and then exported to Microsoft Excel for statistical analysis. Duplicate biological samples were analyzed by LC-MS/MS on an ORBITRAP XL mass spectrometer with three technical replicates using quantitative spectral counting. Centroided ion masses were extracted using the extract_msn.exe utility from Bioworks 3.3.1 and were used for database searching with Mascot v2.2.04 (Matrix Science) and X! Tandem v2007.01.01.1 (www.thegpm.org). Searches were conducted in the

current IPI or SWISS Prot human database using the following search parameters: parent ion mass tolerance 10 ppm; fragment ion tolerance 0.8 Da; and one missed tryptic cleavage. Gln->pyro-Glu of the N-terminus, oxidation of methionine, formyl of the N-terminus, acetyl of the N-terminus and carbamidomethyl of cysteine were specified in Mascot and X! Tandem as variable modifications. Peptide and protein identifications were validated using Scaffold v2.2.00 (Proteome Software) and the PeptideProphet algorithm. Probability thresholds were greater than 99.0% probability for protein identifications, based upon at least 2 unique peptides identified with 90.0% certainty. Proteins that contained similar peptides and could not be differentiated based on MS/MS analysis alone were grouped to satisfy the principles of parsimony. Each ID contains at least four spectral counts on average per technical replicate, and was present in both of the biological samples with significant differences between the control and drug treated cells of $p<0.5$ (T-test).

Antibodies used for Western blotting:

Cul3- ab75851; DBC2 –N15 and C20 Delta Labs; G3BP1- sc-81940; DCP2 – ab28658; TIA-1 – sc-1751; CSN4- NBP1-56646; Hsp90, Hsp70, Hop, cdc37 – lab prepared;

Results

See supplemental attached file: DBC2 Results

Discussion:

The Hsp90 chaperone machine has a plethora of client protein covering most aspects of cellular pathways and functions (current list; www.picard.ch/download/Hsp90interactors.pdf). Steroid hormone receptors (SHR) are a subset of the Hsp90 client proteins that have been extensively studied. The SHR chaperone cycle which modulates the receptor's hormone binding function, begins with the binding of Hsp70 and Hsp40. Then, this complex binds Hop which facilitates the bridging of the SHR to Hsp90. At this point in the cycle the SHR is unable to bind hormone. It becomes competent to bind hormone after the binding of ATP, release of the Hsp70 and Hop, and the recruitment of p23 and the immunophilin FKBP52. Once in this complex the SHR is now ready to bind hormone and begin cellular signaling (Picard 2006). This cycle is similar to the process that DBC2 goes through as it binds to the chaperones Hsp70, Hsp90 and the co-chaperone Hop (Figure 1, 2b, 5e). Additional components of that are involved in the transition from early chaperone complexes to intermediate and late Hsp90 machine complexes are shown in Table 4, which includes Hsp40 (early) and p23 (late) chaperones complexes associated with DBC2 during its interaction cycle (Figure 8).

This study further examined the binding of the chaperone machine in relationship to the domain structure of DBC2. A multi-domain protein, such as DBC2, may contain multiple motifs that require Hsp90-assisted folding. Cdc37, whose interaction with DBC2 initially identified it as a putative Hsp90 client, was also demonstrated to interact with additional motifs within the DBC2 structure. While Cdc37 interacted somewhat weakly with full length DBC2, it was observed to interact with DBC2 deletion mutants extending beyond the Rho domain until the bipartite linker region of the first BTB domain was deleted. This area of the protein is rich in predicted phosphorylation motifs, among others post-translational modifications, with a strong possibility of Cdc37 participating in modulation of these modifications.

The interactions of DBC2 with components of the Hsp90 chaperone machinery indicate that the Hsp90/Hsc70/HOP chaperone module strongly localized to the Rho domain of DBC2.

However, components of Hsp90 chaperone modules containing Cdc37 appear to interact with signaling motifs present distal to DBC2 Rho domain.

The Hsp90's modulation of DBC2's GTP binding suggests that it is not regulated by mechanisms that modulate the classical G-protein GTPase cycle. The classical cycle includes guanine nucleotide exchange factors (GEF), facilitating the exchange of GDP for GTP. GTPase-activating proteins (GAPs) that stimulate the catalysis of GTP to GDP. GDP disassociation inhibitors (GDIs) that impede the replacement of GDP by GTP, and the newly coined GDI displacement factor (GDF) that stimulates the release of the GDI from the G-protein (DerMardirossian and Bokoch 2005).

Atypical small GTPases have been demonstrated to function outside the framework of this classical GTPase cycle (Aspenstrom et al., 2007). The families with characteristics that qualify them as atypical are Rnd, RhoBTB, Wrch-1/Chp, and RhoH (Aspenstrom, Ruusala et al. 2007). They all have in common altered GTP binding/hydrolysis capabilities. For example, Wrch-1 (RhoU) has such a rapid nucleotide exchange rate in the absence of any substitutions within the nucleotide binding consensus sequence, that it is considered to be constitutively bound to GTP (Aspenstrom, Ruusala et al. 2007). Rnd, RhoH and RhoBTB proteins have substitutions in their conserved consensus GTP binding site. However, the RhoH and Rnd proteins have been shown to remain in the GTP bound state, and to lack GTP hydrolysis activity (Aspenstrom, Ruusala et al. 2007). Regulation of the Rnd G-protein is modulated through its degradation which terminates its functional activity (Chardin et al. 2006). This is a mechanism proposed for the regulation of DBC2 function, with the Cul3 ubiquitin ligase system catalyzing the auto-ubiquitination of DBC2 in the absence of bound substrates. The increase and decrease of GTP binding in response to inhibition of the Hsp90 ATPase cycle by molybdate and gelanamycin, respectively,(Figure 4c, d) suggests a functional modulation of GTP binding similar to that by which Hsp90 prepares the hormone binding domain of the SHR to accept hormone (Echeverria and Picard 2010) (Figure 8).

Exemplifying the GTP binding of DBC2 is the desthiobiotin activated GTP cross-linking of biotin to DBC2. The proposed crosslink is to Lys27 of the P-loop, which is also present in the other Rho mutants tested. Each mutant retained the specificity for GTP binding, as well as having their GTP-binding activity modulated by the Hsp90 chaperone machine (figure 5b,d,e). The reduced GTP-binding of DBC2 in the presence of geldanamycin is reminiscent of the Hsp90-bound glucocorticoid receptor (GR) in the presence of geldanamycin (Echeverria and Picard 2010) in which the steroid hormone binding pocket remains inaccessible until Hsp90 progresses to its "late" complex conformation.

The previously reported Cul3:DBC2 interaction was confirmed in this study with an expansion of the DBC2/CRL complex to include its interaction with the regulatory COP9 signalosome. The COP9 signalosome binding to Cul3 is required for the activation and regulation of its E3 ligase activity, and may function to stabilize DBC2 in the absence of Cul3 target proteins, via COP9 deneddylation of Cul3 or direct COP9 mediated deubiquitination of DBC2 (Bosu et al., 2008). Regardless, COP9 signalosome preforms an obligatory function closely associated with the ubiquitin proteasome pathway, which may be linked to the ubiquitinated protein mediator complex formed between COP9, VCP and USP15, and thus it may play a potential role in the sorting of Cul3:DBC2 target proteins (Cayli et al., 2009).

The identification of DBC2-associated E2 ligases (UBE2O, 22% coverage, 23 unique peptides, p=4.4E-16; and UBE2H, 36% coverage, 9 unique peptides, p=4.3E-7) and a HECT E3 ligase (C12orf51, 17% coverage, 68 unique peptides, p=2.0E-35) by LC-MS/MS analysis of DBC2 pull downs, further supports a role for DBC2 as a substrate adapter for ubiquitin ligase complexes. In addition, the Cul4-associated substrate adapter DDB1, and the SKP1/Cul1-associated protein CACBP, which also presumably functions as a substrate adapter, were identified in pull downs of DBC2 from MCF7 lysates. These findings suggest that there may be regulatory crosstalk between Cul3 E3 ligase complexes and the Cul4 and Cul1 E3 ligase complexes, in addition to the hypothetical E3 ligase (C12orf51)(Angers et al., 2006, Wilkins et

al., 2006, Matsuawa et al., 2002). This crosstalk may potentially involve E3 ligase modulated turnover of substrate adapters associated with other E3 ligase systems.

The tolerance to the anti-proliferation effects of DBC2 by resistant HeLa cells can be attributed to sequestration of DBC2 into SGs, a structure that controls both stalled translational pre-initiation complexes that accumulate due to eIF2alpha phosphorylation that occurs in response to stress (Kedersha et al. 2005). The lack of an association of DBC2 with the hallmark PB protein DCP2 indicates that DBC2 is solely present in SGs. Since SGs, like aggresomes, contain aggregates of unfolded and ubiquitinated proteins that are to be target for degradation by the proteasome pathway, the previously reported rapid degradation of DBC2 may stem from DBC2's involvement with SGs as a means of efficient sequestration and subsequent degradation (Brooks et al., 2010; Collado et al., 2007).

The diversity of DBC2 interacting proteins identified in the sensitive MCF-7 cell line play roles in modulating many different areas of cellular function, the Cul3 E3 ligase and the proteasome pathway being previously discussed. DBC2 is known to play a role in the regulation of cellular proliferation. The identification of DBC2 interactions with other cell components will help to connect DBC2 to pathways that modulate cell proliferation, along with the currently recognized effects of DBC2 on CXCL14 and BRSM1 expression, in conjunction with Akt and ezrin phosphorylation (Ling et al., 2010; McKinnon et al., 2008).

The association of DBC2 with additional cellular components involved in cytoskeletal dynamics and vesicular transport along microtubules and with motor proteins is consistent with its reported involvement in the transport of VSVGs from the ER to the Golgi (Chang et al., 2006. The identifications include association of DBC2 with the adaptor proteins AP-2A1, 2B1 and 3B1, connecting DBC2 to cargo protein selection during the formation of vesicles, which may explain DBC2's link to components of the ER based chaperone machinery.

The identification of the presence of ezrin in the DBC2 pull downs supports the interaction of DBC2 deduced by Ling (et al., 2010). DBC2's interaction with the additional ERM

family member, moesin, further supports a role for the interaction of DBC2 with actin filament components at the plasma membrane (Aspernstrom et al., 2004). DBC2/RhoBTB2 expression has been reported to have no effect on the organization of actin filaments. Instead DBC2/RhoBTB2 was found associated with vesicular structures suggesting a possible function in vesicular docking and fusion. Such a role for DBC2 may explain the observation that DBC2's is highly expressed during neurogenesis, suggesting that DBC2 may play a role in modulating synaptic vesicle formation and release, or vesicle trafficking that is required for synaptic pruning and/or growth (St. Pierre et al., 2004; Knowles et al., 2002).

The possible involvement of DBC2 with chromatin remodeling is likely linked to its localization to paraspeckles through it His repeat motif (Salichs et al., 2009). Paraspeckles are known to reside inside the nucleolus in the interchromatin space, and they have been suggested to play a role in transcriptional control: a function that is also connected to the COP9 signalosome (Fox et al. 2010; Chamovitz et al., 2009). The proteins residing inside of paraspeckles have been shown to interact with RNA Pol II, and as such may be associated with active genes (Fox et al., 2002). Whether DBC2's role is the regulation of transcription factors through Cul3 or a novel function controlling actively transcribing genes, but is noteworthy that several of the identified DBC2-associated nuclear proteins have known links to chromatin remodeling.

The following model is proposed for Hsp90 in the modulation of DBC2 that is consistent with the effects of geldanamycin and molybdate on the interaction of Hsp90 chaperone machine components with DBC2, their effect on the binding of GTP to DBC2, aand DBC2's interaction with Cul3 and the COP9 signalosome. The Hsp90 chaperone machine is proposed to function as a molecular wedge that separates the DBC2 Rho domain from an intramolecular interaction with the BTB domain region, an interaction that suppresses its GTP binding activity. Release of DBC2 from its auto-repressed conformation would free the BTB domains for binding to Cul3 and open the Rho domain to GTP binding (Figure 8). This model is consistent with findings that the Rho domain of DBC2/RhoBTB2 interacts with its BTB region, which maintains it in an inactive

state, preventing its ubiquitination and degradation by the proteosome (Berthold et al., 2009). However, the modulation of the GTP binding and domain separation are not the only aspects of the coupling of the Hsp90 cycle to DBC2 function. The Hsp90 chaperone machine also acts as a scaffold for the assembly of DBC2 complexes. Geldanmycin-bound Hsp90 associates with DBC2 in its auto-inhibited conformation, which is lacking in GTP and Cul3 binding. Progression of the Hsp90 to the intermediate stage of its cycle releases DBC2 from its repressed conformation stimulating the binding of GTP and DBC2's interaction with Cul3. The subsequent release of the Cul3-DBC2 complex from the Hsp90 chaperone machine allows components of the COP9 signalosome to assemble into the Cul3/DBC2 E3 ligase complex. It is not known whether neddylation of Cul3 occurs prior to its release from Hsp90, but the association of the core signalosome component CSN4 subunit with molybdate stabilized Hsp90/DBC2 complexes suggest it may occur while Cul3 is bound at the late stage in the Hsp90 cycle. Thus, DBC2 must transit the entire Hsp90 ATP-driven reaction cycle for it to reach its full signaling potential. Whether Hsp90 facilitates DBC2's assembly into additional non-Cul3 containing complexes, which function in other noted pathways, or whether these components are target of Cul3/DBC2 E3 ligase complexes needs further investigation.

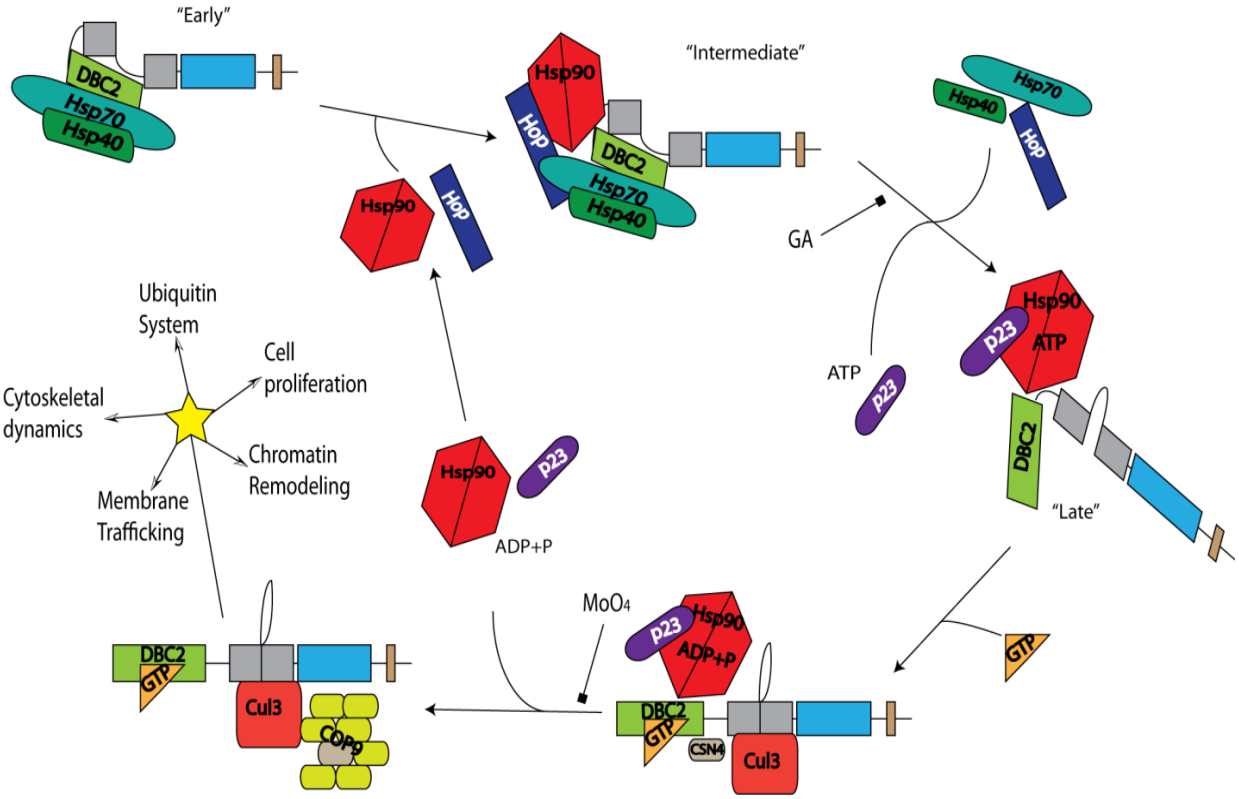

Figure 8. **A representative model for the integration of the Hsp90 ATPase cycle with the modulation of DBC2 GTP binding/activation.** The DBC2 domains are: 1) Rho domain, 2) BTB1 domain, 3) BTB2 domain, and 4) putative RING domain. The (x) is in reference to the Rho domain that is not competent to bind GTP. "Cul3" and "CSN4" are used as example proteins whereas they can represent any know associating proteins. "Early", "intermediate", and "late" refer to the Hsp90 ATPase cycle formed complexes.

CHAPTER III

Wheat Germ Lysate a Cdc37 Null System

Introduction

The Hsp90 chaperone machine interacts with many co-chaperone partners that are required for its interaction with client proteins and chaperoning function, providing it with the ability to serve a diverse set of clientele. Cdc37 was first identified in 1980 as a protein involved in control of the cell cycle and was subsequently found to be what is coined the "kinase specific" co-chaperone of the Hsp90 chaperone machine (Reed et al. 1980; Schulz et al. 2001). Cdc37 was designated the kinase specific co-chaperone due to its interaction with Hsp90 protein complexes containing protein kinases clients, but its absence from Hsp90/ steroid hormone receptor complexes(Schulz et al. 2001). A list of Cdc37 interacting proteins can be found at (www.picard.ch/download/cdc37interactors.pdf). However, subsequently a specific interaction between Hsp90 and the androgen receptor was demonstrated, suggesting that Cdc37-associated clientele may extend beyond its interaction with protein kinases (Roe et al., 2001).

Phosphorylation of serine 13 (Ser13) has been demonstrated to be necessary for the formation of Hsp90/Cdc37/kinase complexes (Shao et al., 2003). Subsequently it has been proposed that Cdc37 undergoes a cyclic regulatory phosphorylation and dephosphorylation of Ser13 which is involved in the initial assembly and disassembly of the Hsp90:kinase:Cdc37 complexes, respectively (Vaughan et al., 2008). Cdc37 is composed of three functional domains,

the N-terminal kinase binding domain, the middle Hsp90-interacting domain and a C-terminal domain of unknown function (Shao et al. 2003).

Amino acids present in the first eight residues of Cdc37 are highly conserved and have been demonstrated to be critical for the interaction of Cdc37 with protein kinases (Shao et al. 2003). Additional residues, although not clustered in the primary sequence, are also highly conserved raising the question as to their contribution to Cdc37's molecular function. Recently it has been proposed that Cdc37's function is modulated by other post-translational modifications. However, Cdc37 has been shown to dimerize, such that the formation of a mutant/wild-type heterocomplex would have the possibility of masking the effects site-specific mutations designed to test the importance of these conserves amino acid residues in modulating Cdc37 function.

Thus, the identification of a Cdc37 null system to assess the functional consequences of mutations to Cdc37 would be a substantial leap towards deciphering structure/ functional relationships that regulate Cdc37. We have identified the Wheat germ lysate (WGL) system to be Cdc37 null, and demonstrate that it represents a useful model system to explore Cdc37 function and its mechanism of action.

Experimental Procedures

Wheat germ In vitro coupled transcription/translation (TnT):

Each protein construct was synthesized by coupled transcription/ translation (TnT) in WGL (SP6 Quick TnT® Quick Master mix, Promega) supplemented with either [^{35}S]-methionine for 2 H at 25°C in the presence or absence of 10 μg/mL GA, DMSO, 20 mM sodium molybdate (MoO4), deionized water, recombinant p23, recombinant, or casein kinase II (CKII, Cell signaling). Naïve WGL containing no template DNA was used as the control for nonspecific binding.

Nickel (Ni) NTA pull-down assays:

All samples were placed on ice, and then clarified by centrifugation for 12.5 min at (16,000 x g) prior to the pull-down. Samples were added to 15 μl Ni NTA resin, incubated with resin for 1 H at 4°C with mixing, and then washed four times with either low salt buffer containing, 10 mM Pipes (pH 7.4), 300 mM NaCl, 0.5% Tween 20, and 15mM Imidazole (P300T + 15mM imidazole). Samples were then boiled in SDS sample buffer, and analyzed by SDS-PAGE on a 10% gel, followed by electrotransfer to PVDF membrane (BioRad.) and analysis by autoradiography and Western blotting for co-adsorbed proteins. The plant Hsp90 and p60 (Hop) antibodies were provided by Priti Krishna as was the CTR1 construct (AC101-CTR1).

Tyrosine kinase assay:

His-tagged Lck was generated by TnT in WGL in the presence or absence of Cdc37 supplementation with or without the addition of geldanamycin, followed by pull-down with Ni NTA resin as described above. The activity of affinity isolated Lck kinase was determined incubation of resins with 0.5 μg/ml acid-denatured enolase and 1.0 mM ATP (normalized) in buffer containing 10 mM Pipes, pH 7.4, 150 mM NaCl and 20 mM $MgCl_2$ at 22°C for 5 min. Boiling SDS sample buffer was added to the reaction. Then samples were separated by SDS-PAGE and electrotransfered to PVDF followed by Western blotting for Tyr phosphorylation (anti-phosphotyrosine antibody, P-Tyo-100, Cell Signaling, #9411) to visualize enolase

phosphorylation. Co-adsorption of Hsp90 and HOP were analyzed by Western blotting and Cdc37 binding was determined by autoradiography.

Results

Conserved Cdc37 residues

The first 60 amino acids of Cdc37 are the most conserved across multiple species, suggesting that the residues play crucial roles in Cdc37's structure and function (Figure 1). These residues reside inside the kinase binding domain with the function of residues 2-8 of Cdc37 having been tested by scanning alanine mutagenesis for their ability to bind Hsp90 and facilitate the maturation of protein kinases (Shao et al, 2003). In addition, Ser13 has been demonstrated to be necessary for the formation of a ternary complex between Hsp90, Cdc37 and protein kinase. The mutagenesis of other conserved Cdc37 residues would further elucidate molecular mechanisms involved in kinase binding and maturation by the Hsp90/Cdc37 chaperone machinery. As noted in the introduction, the propensity of Cdc37 to forms dimers makes interpretation of experiments in Cdc37-expressing cell system equivocal. Thus, the identification of a system that is Cdc37 null would facilitate structure/ function relationships that govern Hsp90/Cdc37 modulated folding and activation of associated protein kinases.

Cdc37 the missing component

Analysis of the genomes of diverse species for genes encoding Hsp90 co-chaperones found no evidence for a gene encoding Cdc37 in plants (Johnson and Brown, 2009). Therefore, we examined the well-characterized WGL system for its ability to reconstitute the binding of Hsp90 to newly synthesized protein kinase. The *A. thaliana* protein kinase CTR1 was synthesized by coupled transcription/ translation in WGL. Western blotting of pull downs of the newly synthesized His-tagged CTR1 indicated that no Hsp90 was bound to the protein kinase (Fig. 2, lane #). The WGL was then reconstituted with components that we have previously demonstrated to be required for complex formation or that are present in complexes formed between Hsp90 and protein kinase synthesized in rabbit reticulocyte lysate (RRL) (Cdc37, CKII,

and p23), to determine the component was the necessary to restore the presence of Hsp90 in complex with the kinase CTR1. The results presented in Figure 2 demonstrate that without the addition of Cdc37 the ternary Hsp90:CTR1:hCdc37 does not form. In the absence of Cdc37, the amount of Hsp90 that was present in CTR1 pull down was equivalent to that present in the non-specific binding control. Addition of CKII and/or p23 was not sufficient to restore the ternary complex. Furthermore, addition of either p23 or CKII did not enhance the formation of this complex, consistent with homologues of these proteins being expressed in plants (Johnson & brown 2009) (Laxminarayana B, Krishna VM, Janaki N, Ramaiah KV, 2002). Similar to the RRL system, the addition of molybdate was not necessary to stabilize the formation of the Hsp90/ hCdc37CTR1 complex. Thus, the only factor that affects the complex formation in WGL is Cdc37, as it was necessary and sufficient to restore the Hsp90/Cdc37/kinase ternary complex (Figure 2).

The effect of geldanamycin on the reconstitution of the Hsp90/Cdc37/kinase complex.

To determine whether the Hsp90/ Cdc37/ kinase ternary complex that was reconstituted in WGL had properties similar to those of the mammalian RRL system, we examine the effect of the Hsp90 inhibitor on the formation of the ternary complex. In the RRL system geldanamycin prevents the formation of a stable complex between nascent kinases, Hsp90 and Cdc37 (ref). (figure 3). The ternary complex reconstituted by the addition of hCdc37 responded to geldanamycin-inhibition in a manner similar to the complex formed in RRL. The presence of geledanamycin disrupted the interaction of hCdc37 with Hsp90/CTFR1, preventing the formation of the complex (Figure 3, lanes 7-9).

The influence of p23 on the autophosphorylation of the Hsp90 dependent kinase Lck in WGL

To determine whether the addition of p23 would enhance the binding of Hsp90/Cdc37 to the human Hsp90-dependent kinase Lck in WGL and affect its auto-phosphorylation, Lck was

synthesized in the presence or absence of p23 in the presence of Cdc37. No significant enhancement of Hsp90/Cdc37 binding or auto-phosphorylation of Lck was observed upon addition of human p23 to WGL (Figure 4). Thus, wheat germ ortholog of p23 is functional and present in adequate supply, further supporting the conclusion that the only limiting factor in reconstitution of Hsp90/kinase complexes in WGL is Cdc37 (Figure 4).

Hsp90-dependent activation of Lck in WGL

To test the utility of the WGL system for studying the Cdc37-dependent stabilization of the interaction of Hsp90 with protein kinase, the Hsp90-dependent client kinase Lck was generate in the presence or absence of hCDC37 by TnT in WGL with and without the addition of geldanamycin. The properties of Lck generated in WGL was similar to the properties Lck exhibits when synthesized in RRL (ref). The supplementation with Cdc37 was necessary for the for the reconstitution of stable Hsp90 binding to Lck (Fig.5). However, in the absence of hCdc37, Lck kinase was active in phosphorylating the model substrate acid-denatured enolase *in vitro*, and geldanamycin had minimal inhibitory effect on Lck's kinase activity (Fig. 5). Supplementation of WGL with Cdc37, stabilized the binding of Hsp90 to Lck, and stimulated Lck's kinase activity as measured by phosphorylation of enalose. The addition of geldanamycin blocked Hsp90/Cdc37/Lck complex formation and the ability of hCdc37 supplementation to stimulate Lck's kinase (Fig. 5). Western blot analysis of the Lck pull downs indicated that the Hsp90 co-chaperone Hop was specifically bound the Lck and that interaction was not disrupted by addition of geladanmycin or supplementation with hCdc37 (Fig. 5). In non-plant systems, the stable interaction of HOP with protein kinases has not been observed.

Alignment of the Kinase binding domain of Cdc37

Figure 1. **Sequence alignment of the first 60 amino acids of Cdc37 from various organisms**. H.s (Homo sapiens- sp_Q16543), M.m (Mus Musculus- Q61081), B.t (Bos Taurus- sp_Q5EAC6), R.t (Rattus norvegicus- sp_Q63692), S.s (Sus scrofa- tr_Q684M6), G.g (Gallus gallus- sp_O57476), C.e (Caenorhabditis elegans- sp_O02108), C.b (Caenorhabditis briggsae- tr_A8X3Q4), B.m (Bombyx mori- tr_Q5CCL4), X.t (Xenopus tropicalis- tr_Q28CE8), D.r (Danio rerio- tr_Q7ZV56), T.f (Tetraodon fluviatilis- sp_Q9DGQ7),S.sa (Salmo salar- tr_B5X4J1), L.s (Lepeophtheirus salmonis- tr_C1BSQ2), S.j (Schistosoma japonicum- tr_C7TQQ3), D.m (Drosophila melanogaster- tr_Q86NM8), A.f (Aspergillus fumigates- tr_Q4WPP7), S.p (Schizosaccharomyces pombe- sp_O94740), S.c (Saccharomyces cerevisiae- sp_P06101), C.g (Candida glabrata- tr_Q6FVL7), C.d (Candida dubliniensis- tr_B9WIX2), C.a (Candida albicans- sp_Q8X1E6). The large box encases residues 2-8 of the *Homo sapiens* Cdc37 protein along with the aligned residues of the various species, these residues were analyzed by alaine scanning mutatgenesis. The small box indicates the invariant serine residue, which is critical to the function of Cdc37 in the Hsp90 chaperone machinery, also were analyzed with an alanine (A) and glutamic acid (E) substitution via site-directed mutagenesis. Representative labeling, (*)- denotes an invariant residue, (:)- denotes a conserved substitution, (.)- denotes a similar substitution, (sp)- Swiss-Prot and (tr)- TrEMBL.

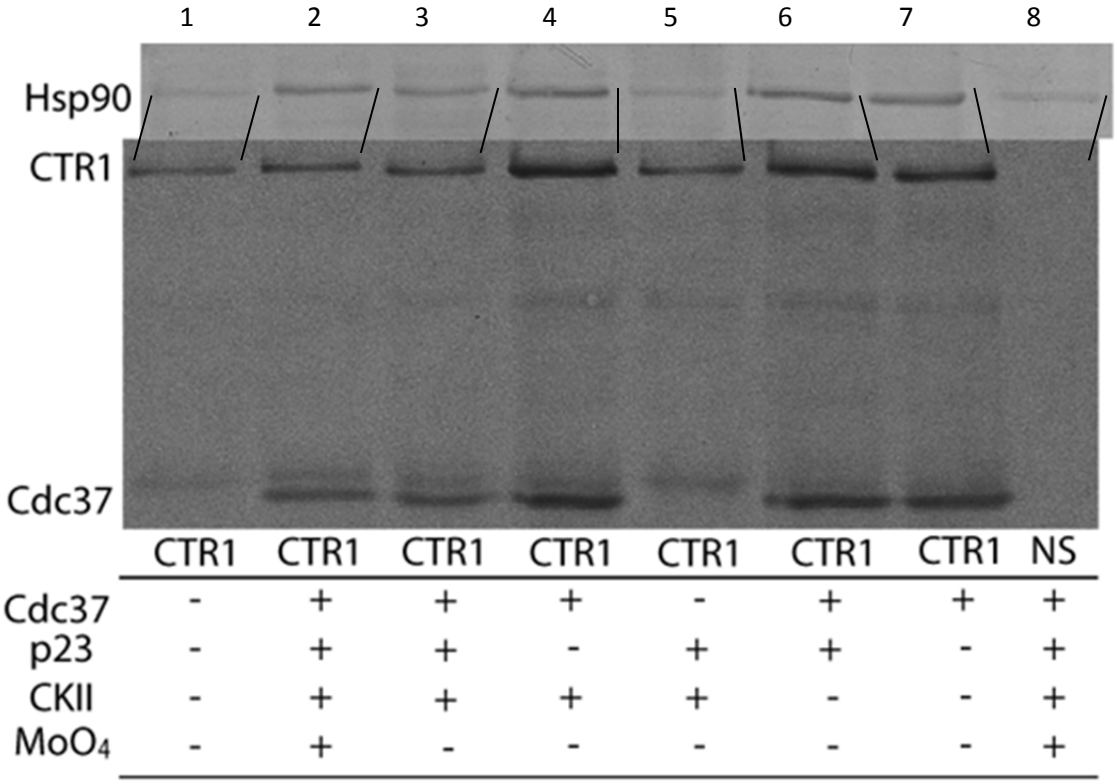

Figure 2. **Co-chaperone-dependent reconstitution of Hsp90 protein kinase binding in WGL**. [^{35}S]Labeled His-tagged CTR1 and hCdc37 were synthesized in WGL in the presence or absence of Cdc37, p23, CKII and MoO4 and pull-down using Nickel NTA resin followed by washing 4 times using P300T with 15 mM Imidazole. CTR1 and Cdc37 (bottom panel) were analyzed through an autoradiogram with Western blotting for plant Hsp90 (top panel). Lane 1 contains only ^{35}S labeled CTR, 1, 2, 3, 4, 6, 7 contain cdc37, lanes 2, 3, 5, 6 all contain p23 with or without cdc37, lanes 2, 3, 4, 5 contain CKII, lane 2 contains MoO_4 and NS lane 8 contains all additives except for the 35S labeled His-tagged CTR1.

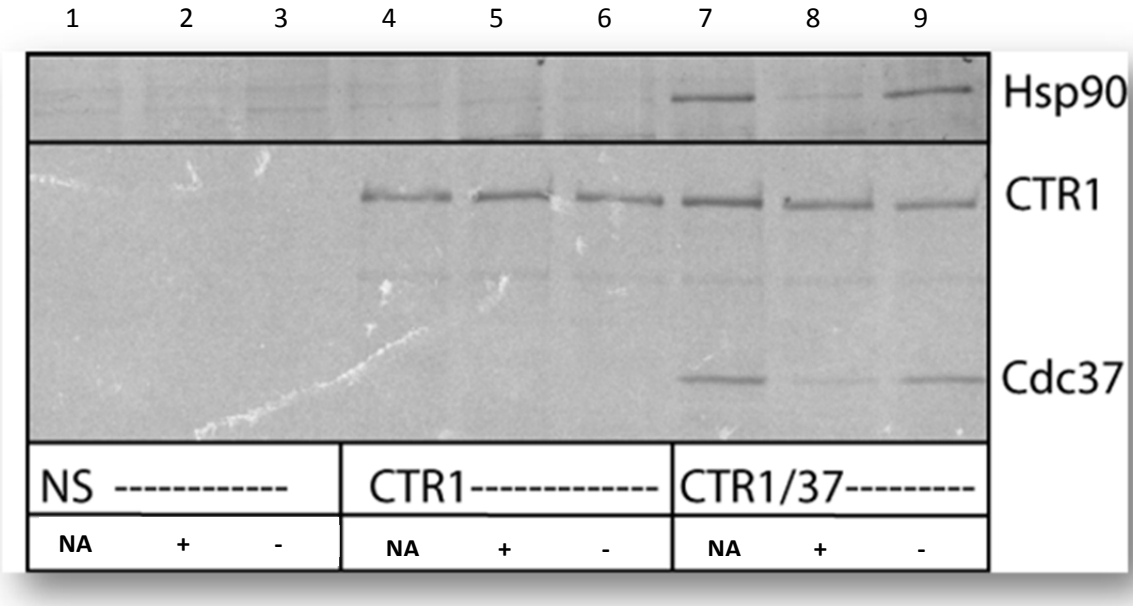

Figure 3. **Ternary complex response to GA inhibition**. . ^{35}S-met labeled His-tagged CTR1 and hCdc37 were synthesized in WGL in the presence or absence of DMSO or GA and pull-down using Nickel NTA resin was followed by washing 4 times using P300T with 15mM Imidazole. CTR1 and cdc37 (bottom panel) were analyzed through an autoradiogram with western blotting for plant Hsp90 (top panel). Lanes (1-3) represent the NS Translation and binding control, lanes (4-6) are only CTR1 without the addition of translated hCdc37 and lanes (7-9) contain CTR1 with the addition of translated hCdc37. Lanes (2, 5, 8) all contain the Hsp90 inhibitor GA (+) while all additional lanes either have DMSO (-) or No addition (NA).

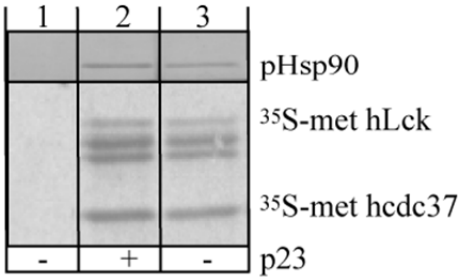

Figure 4. ^{35}S-met labeled His-tagged hLck and no tag hCdc37 were synthesized in WGL in the presence or absence recombinant p23 followed by a pull-down using Nickel NTA resin and washed 4 times using P300T with 15mM Imidazole. hLck and cdc37 (middle panel) were analyzed through autoradiogram with western blotting plant Hsp90 (top panel). Lane 1 is the NS control, lane 2 is supplement with recombinant p23 and lane 3 is without.

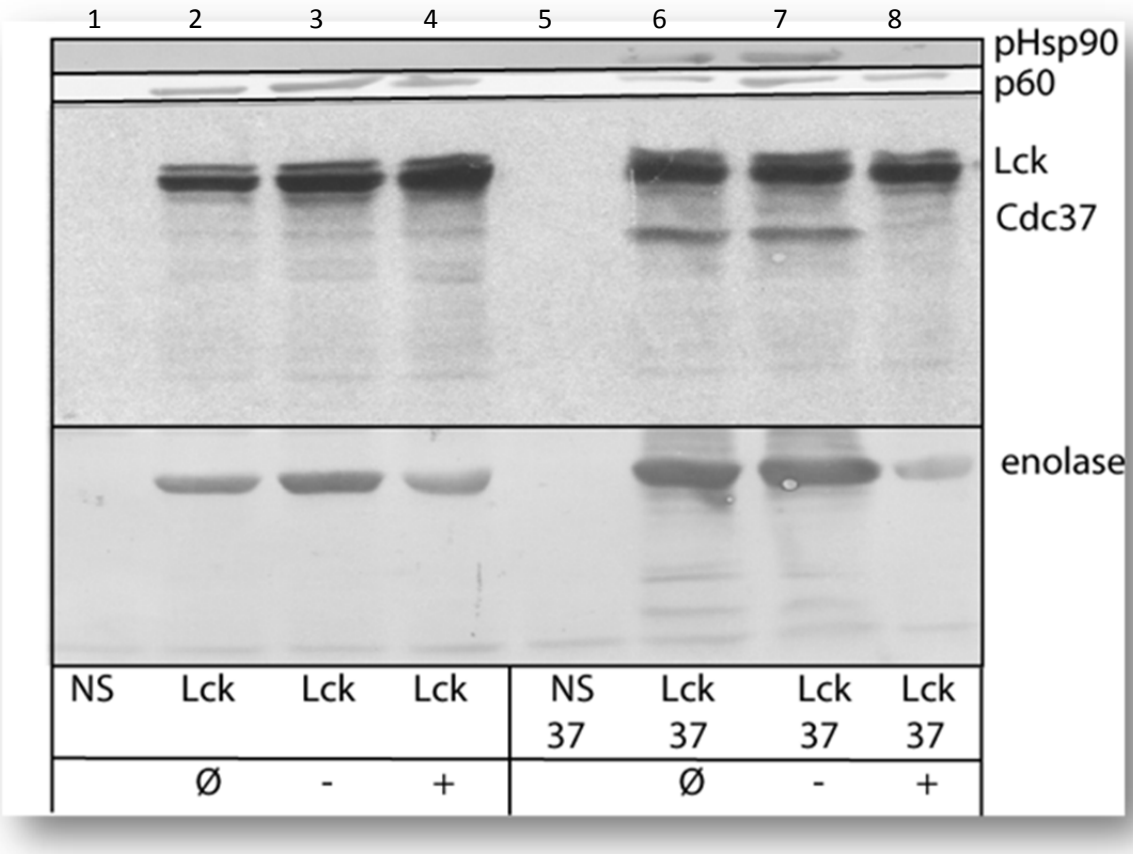

Figure 5. **The response to GA inhibition along with activation with hLck in WGL**. . ^{35}S-met labeled His-tagged hLck and hCdc37 were synthesized in WGL in the presence or absence of DMSO or GA and pull-down using Nickel resin was followed by washing 4 times using P300T with 15mM Imidazole. hLck and cdc37 (middle panel) were analyzed through autoradiogram with western blotting plant Hsp90 and p60 (Hop) (top panel). Testing the activity of the hLck synthesized in WGL in the presence and/or absence of GA and cdc37 and western blotted Tyr phosphorylation of enolase (Y100) (bottom panel). Lanes (1, 5) represent the NS translation and binding control, lanes (2-4) are only hLck without the addition of translated hCdc37 and lanes (6-8) contain hLck with the addition of translated hCdc37. Lanes (4, 8) all contain the Hsp90 inhibitor GA (+) while lane (3, 7) either have DMSO (-) or lanes (2, 6) No addition (Ø).

Discussion

The kinase binding domain of cdc37, containing the most highly conserved sequence, has the ability to supplement and maintain yeast viability when Hsp90 function is deficient or in the absence of Sti1 (the yeast Hop homolog) (Lee et al., 2002). The functionality is attributed to the inherent chaperone function associated with Cdc37 even in the absence of its association with Hsp90 (Lee et al., 2002). Cdc37's Hsp90 binding domain interacts with Hsp90's N-terminal domain and blocks its ability to bind and hydrolyze ATP during the client loading phase of the Hsp90 ATPase cycle (Roe et al, 2004). Structure/function relationships that govern Cdc37's binding to Hsp90 and kinase and its ability to support kinase maturation are of great interest because of the oncogenic nature of many of its substrates, along with the oncogenic properties of the over-expression of Cdc37 itself (Pearl et al., 2005). The presence of Cdc37 is essential for viability in yeast, *Drosophila* and *Caenorhabditis elegans* (MacLean et al., 2003), making the identification of a Cdc37 null system, such as wheat germ lysate (WGL), a significant technical stride. Structure/ function relationships governing Cdc37's activities can now be studied without interference of a background expression of wild-type Cdc37, circumventing the problem that might arise due to Cdc37 dimerization and the formation of wild-type/ mutant Cdc37 heterocomplexes that may potentially mask the effect of the mutation (Roiniotis et al., 2005).

Cdc37 was identified as the co-chaperone that was necessary and sufficient to reconstitute the Hsp90: kinase complexes in WGL, consistent with the observation that Cdc37 is essential in promoting the formation of Hsp90/kinase complexes in other eukaryotic cell systems (Smith et al., 2008). The reconstituted WGL/Cdc37 was found to have properties similar to those of RRL, with the Hsp90 inhibitor geldanamycin disrupting the binding of Hsp90 and Cdc37 to the Arabidopsis Ser/Thr kinase CTR1 and to the human Lck tyrosine kinase.

Of interest, however, is the observation that the Lck kinase expressed in WGL has significant kinase activity in the absence of supplementation of the lysate with Cdc37. While Cdc37 supplementation stabilized the binding of Hsp90 and Cc37 to Lck and stimulated Lck's tyrosine kinase activity, Lck's maturation was not entirely contingent on the presence of Cdc37. The stimulation of Lck's kinase activity was due to the presence of Cdc37, as this stimulation was lost upon addition geldanmycin. Curiously, a stable association of HOP with Lck was observed both in the presence and absence of geldanamycin, and the interaction was not inhibited in the presence of Cdc37. These observations suggest that HOP may function in kinase maturation in the plant system in lieu of Cdc37. While an interaction of HOP with protein kinases have not been observed in mammalian cell systems, Sti1 (yeast HOP) has been demonstrated to play a role in stabilizing Hsp90/kinase complexes in yeast (Lee et al 2004). Thus, in addition to its utility in studying structure function relationships that regulate Cdc37, the WGL system may also facilitate studies examining the role of Sti1/HOP in kinase maturation which may occur in other eukaryotic cell systems, particularly the Plasmodium and Trypanasomal pathogens which have a gene coding for a HOP homologue, but no gene coding for Cdc37.

CHAPTER IV

The Direct Binding of Novel Small Molecule inhibitors of Hsp90

Introduction

Surface Plasmon Resonance, (SPR,) is an optical technology able to detect direct interactions of biomolecules as the mass changes on the sensor surface. SPR has gained popularity in the biomedical industry mainly due to the development and optimization of both the instruments and methods, in the field over the past two decades (Thillaivinayagalingam et al. 2010.) The tremendous strides into the identification and characterization of direct interactions of biomolecules with ligands, whether the ligand is a protein or a small molecule has made this technology more attractive to the academic sector as well as industry. The SPR technology along with a nano-scale flow system reaches further towards replacing the high reagent consuming coupled enzymatic reactions previously used to determine the kinetics of a reaction. This label-free real time method allows for the binding and dissociation kinetics to be calculated with more certainty, and thus binding affinities have more accuracy then those previously gathered. All information reviewed in Shiau et al., 2008; Rich et al., 2008; Thillaivinayagalingam et al., 2010; Merwe; Bokatzian-johnson, 2008.

SPR detection is based on ability to generate surface plasmons at the interface of materials that differ in refractive index. The generation of surface plasmons begins with a beam of plane polarized light directed at back of the sensor surface which results in an evanescent wave

exciting the electrons in the gold coated sensor surface that is in direct contact with the assay medium on the other side of the glass surface. This in turn causes a change in the strength of the reflected light. When the refractive index at the surface of the sensor is changed, the angle of reflected light is altered which is known as a resonance signal. This resonance signal is directly proportional to the change in mass at the sensor surface caused by the binding of the analyte to the immobilized ligand and is recorded as response units (RU) which corresponds to the shift of the measured angle (Figure 1.)

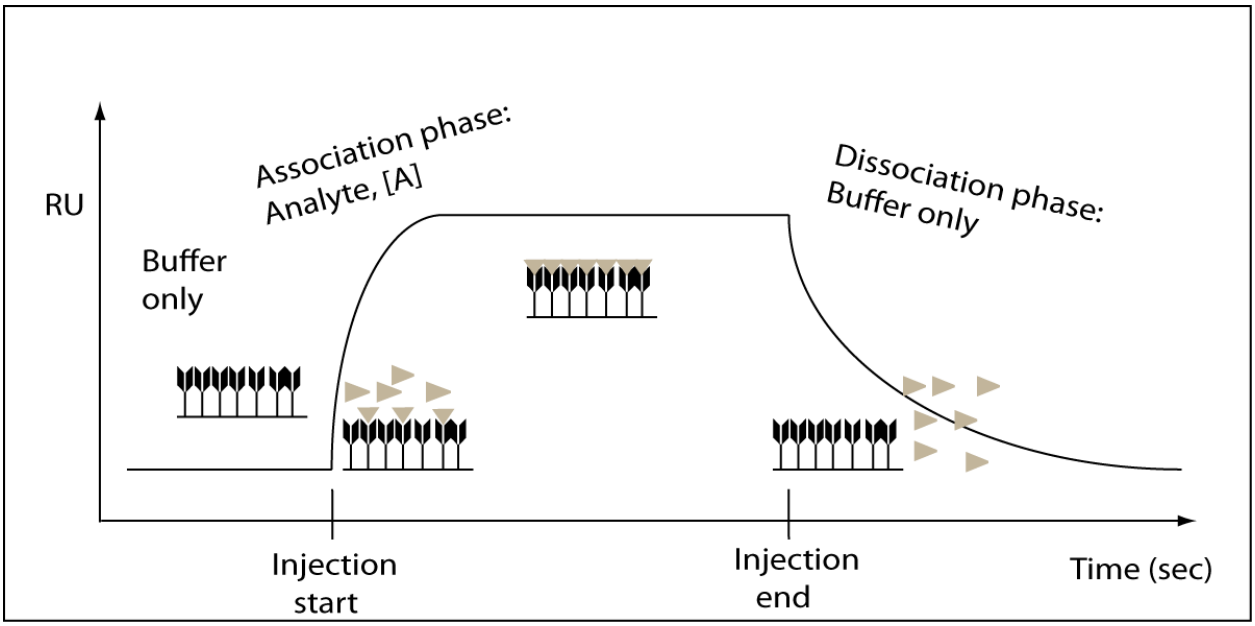

Figure 1: **Theoretical sensorgram depicting a SPR data collection run.** Inserts show the composition and arrangement of ligand and analyte at each phase of the sensorgram. Black flags represent immobilized ligand and grey triangles represent the injected analyte.

SPR in terms of a bimolecular application begins with surface chemistry that is applied to the gold coating on the sensor surface. This begins with the application of a layer of molecules to ensure proper spacing between the biomolecules and the gold surface, but also carries a carboxylic acid group for subsequent reactions. There are many different variations for the next layer, but for this example we with explore a covalent immobilization (amine coupling) and the capture approach (NeutrAvidin:biotin.) The first is considered to be the most popular, and involves immobilization of a protein through free primary amines. First the carboxylic acid groups on the surface of the sensor are activated to which the protein of interest is then covalently linked. After the quenching of any free reactive group generated that remain on the sensor's surface, the sensor is ready for data acquisition. The second method begins with covalent amine coupling of Neutravidin to the sensor surface as mentioned above, but the protein (ligand) of interest is not directly immobilized to the sensor surface. The protein is first derivatized, in this case with the addition of a biotin for capture by the surface immobilized Neutravidin.

The next steps are both consistent for each of the methods of protein capture. The analyte at multiple concentrations is injected over the protein (ligand) bound sensor surface with the RUs recorded in real time being the result of ligand-analyte interaction. This measurement allows for the accurate kinetic information to be derived in real time for the reasons mentioned above.

There are many advantages to this method: it is label free; it continuously monitors kinetic events (the binding and dissociation of the analyte from the ligand); and it allows for the analysis of a large number of samples. As for all methods there are some disadvantages as well that could pose a problem: sufficient amounts ligand must be immobilized to reproducibly detect a signal; the ligand/ chip linkage in the analyte buffer must be robust; and the stability of the immobilized protein used for the assay. There are methods to ensure and/or test for each of these disadvantages during the assay development for each particular experimental setting. All of these

factors must to be taken into consideration before it can be ascertained whether SPR can be used to address a given experimental question. With all the powerful features that SPR has it is surely to become a common technology utilized in the years to come. All information reviewed in Shiau et al., 2008; Rich et al., 2008; Thillaivinayagalingam et al., 2010; Merwe; Bokatzian-johnson, 2008.

Experimental Procedures

Surface Plasmon Resonance (SPR):

SPR experiments were performed on the ICX, Nomadics SensiQ instrument using Hamilton syringes for injection of assayed materials. All measurements were done in triplicate and SPR binding curves were analyzed using QDAT software (ICX Nomadics) to calculate the k_a, k_d,and K_D data.

Protein binding buffer consisted of 10 mM Hepes buffer (pH 7.4) containing 150 mM NaCl. Sample and assay running buffer contained 10 mM PIPES (pH 7.4), 300 mM NaCl, and 2% DMSO or 5% DMSO. The N-terminal Hsp90 construct (Hsp90NT) corresponded to amino acids 1-241 with a C-terminal-GELRSGC tail due to a pET151 TOPO 3' vector extension. The C-terminal Hsp90 construct (Hsp90CT) corresponded to amino acids 531-732

Protein preparation:

Insect Sf9 cells overexpressing human Hsp90β were cultured and harvested by the Baculovirus/Monoclonal Antibody Core Facility at Baylor College of Medicine and purified according to Grenert et al. (1997) and Owen et al. (2002.) However, the initial DEAE-cellulose chromatography step was omitted.

Bacterial expressed His-tagged full length Hsp90 (Hsp90FL), Hsp90NT and Hsp90CT were grown in DE3 star E.coli and purified using a NiNTA affinity column, followed by cleavage of the N-terminal His-tag by TEV protease (Invitrogen) after purification. Following epitope tag cleavage the proteins were further purified by size-exclusion on a Superdex 200 column.

Bacterial or Sf9 expressed purified recombinant proteins were passed through a desalting column (BioEdge) into a buffer containing10 mM HEPES (pH 7.4) and 150 mM NaCl to prepare the proteins for immobilization to a COOH sensor surface. For immobilization on Neutavidin

sensor chips, proteins were biotinylated by reaction with EZ-Link® Maleimide-PEG_2-Biotin (Thermo Scientific) according to manufacturer's protocol, followed by passage through a desalting column (BioEdge) into buffer containing 10 mM HEPES (pH 7.4), and 150 mM NaCl to prepare them for binding to Neutavidin.

Protein immobilization:

Sensor normalizations were carried out using protocols developed by Dr. Shawn Daley and Ms. Kristen Szabla (OSU Biochemistry and Molecular Biology department) in conjunction with ICX, Nomadics. This method was developed through personal communication and interaction with Dr. Shawn Daley.

Proteins were immobilized on COOH sensor chip surfaces as follows: The surface of a SSO1 COOH sensor chip was normalized and activated by treatment with N′-3-dimethylaminopropyl-N′-ethylcarbodiimide hydrochloride and N-hydroxysuccinimide for preferential cross-linking of full-length Hsp90s N-terminus to the surface. For immobilization of Hsp90, 250 µL of Hsp90 (6.2 mg/mL) in 10 mM Hepes buffer (pH 7.4) containing 150 mM NaCl was discrete-injected over the sensor's experimental surface at a flow rate of 5-10 µL/min, resulting in 2000 response units of protein captured. Then, 1 M ethanolamine (pH 8) was used to quench the remaining activated groups, and the surface subsequently washed with assay running buffer.

The surface of a SSO3 BioCap SPR sensor chip was mounted in a SensiQ SPR instrument (ICX Nomadics), and either the biotinylated Hsp90NT (7.0 mg/mL) or Hsp90CT (6.8 mg/mL) was discrete-injected over the experimental channel at a flow rate of 5-10 µL/min, resulting in the capture of Hsp90NT and Hsp90CT at 1250-1400 response units of protein on the sensor experimental surface, respectively. The sensors were subsequently washed with assay buffer prior to experimental analysis.

The various compounds were diluted in assay running buffer containing 10 mM PIPES (pH 7.4), 300 mM NaCl, and 2% DMSO and injected over the surface of each protein bound sensor at a flow rate of 15 μL/min at 25°C at the indicated concentrations. The dilutions of all compounds were specifically matched to the assay running buffer to minimize index shifts induced by the DMSO. Curves were double referenced to subtract contributions of the buffer containing 2% DMSO to the response units.

Competitor solutions

Geldanamycin competition studies were conducted using a constant 20 μM concentration of geldanamycin in the sample and running buffer. The concentrations of Gambogic acid were varied as indicated by dilution into assay running buffer containing constant 20 μM GA.

Results and Discussion

KU174

Interaction of KU174 with Hsp90β was analyzed by surface plasmon resonance (SPR) spectroscopy. KU174 is a proprietary compound designed by the laboratory of Dr. Brian Blagg from the University of Kansas. Various concentrations of KU174 were injected over Hsp90FL bound to the sensor surface (Fig. 2). The response units generated during the injections illustrated that KU174 directly interacted with Hsp90 (Fig.2A). The kinetics of KU174 binding to and dissociating from Hsp90 were reliably fitted to a pseudo-first order model for a 1:1 interaction with the k_a and k_d calculated to be $1.04x10^3$ ($M^{-1}\cdot sec^{-1}$) and 0.098 (sec^{-1}), respectively. The K_d estimated from the fitting of the binding curve (Fig. 1B: 78 μM ± 7 s.e.) was in close agreement with the K_d estimated from the ratio of the dissociation and association constants (94 μM ± 4 s.e.). In comparison, the k_a and k_d for the binding of novobiocin to Hsp90β were 211 ($M^{-1}\cdot sec^{-1}$) and 0.23 (sec^{-1}) (calculated K_d of 1.1 mM ± 0.4 s.e), with a K_d calculated from the binding curve of 0.86 mM ± 0.02 s.e.). Thus, the SPR analysis of the interaction of KU174 with Hsp90β indicated the compound bound directly to the purified recombinant protein with a reasonably high affinity in vitro (Eskew et al., 2011).

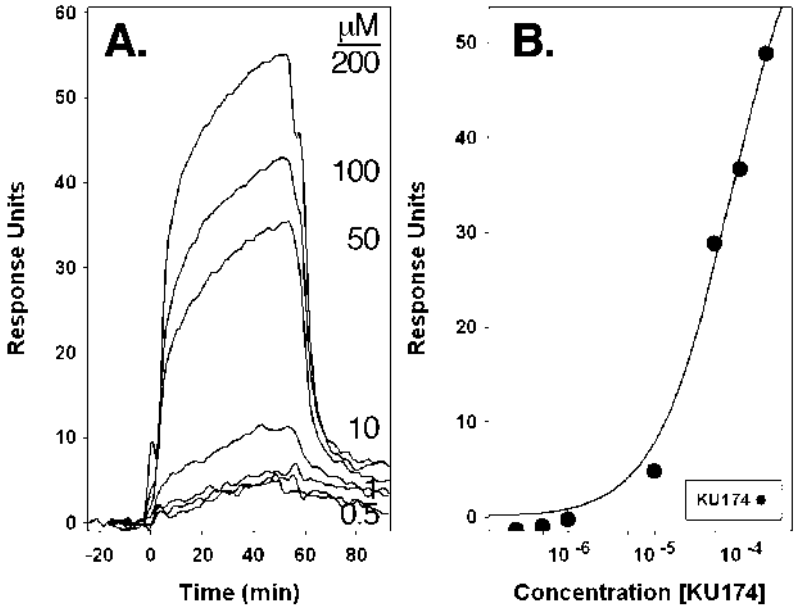

Figure 2. **Anaylsis of the binding of KU174 to Hsp90β by SPR**. KU174 was injected over Hsp90β immobilized to the surface of a SPR sensor chip at concentrations of 0.25, 0.5, 1.0, 10, 50, 100, and 200 μM as described under "Materials and Methods". (**A.**) Sensorgrams of KU174 binding to Hsp90β. (**B.**) Concentration dependent binding curve for the interaction of KU174 with Hsp90□.

Gambogic Acid:

Gambogic acid (GBA-appendix A) was identified through a high throughput screen of a natural product library for inhibitors of Hsp90-dependent refolding of thermally denatured firefly luciferase. In vitro studies indicated that GBA functions similarly to known Hsp90 inhibitors (e.g GA-appendix A, Davenport et al, 2011), inhibiting the Hsp90-dependent maturation of the heme-regulated eIF2 alpha kinase (HRI) and blocking the interaction of HRI with Hsp90 and its co-chaperone Cdc37. SPR was carried out to determine if GBA interacted directly with Hsp90 and whether GBA binding was localized to Hsp90's N- or C-terminal domain.

Hsp90FL showed a strong response to the presence of GBA (Figure 3) indicating that GBA interacted directly with Hsp90. To determine which domain the GBA binding site, Hsp90NT and Hsp90CT were analyzed for their ability to interact with GBA. Hsp90NT was found to bind to GBA with an affinity similar to Hsp90FL, with no measurable response being detect with GBA was inject over the immobilized HSP90CT sensor surface.

To determine whether GBA bound to the same site in Hsp90NT as GA, GBA was injected over the sensor surface in the presence of a constant 20 μM concentration of GA in both the assay and sample buffer. GA did not have any significant effect on the binding of GBA to Hsp90NT, with the calculated GBA binding affinity being comparable to that of GBA binding in the absence of a nucleotide binding cleft competitor (Table 1). Thus, GBA appears to bind to a novel Hsp90 N-terminal domain binding site, as GA, a known nucleotide binding cleft inhibitor, had no effect on GBA binding and/or affinity (Davenport et al., 2011).

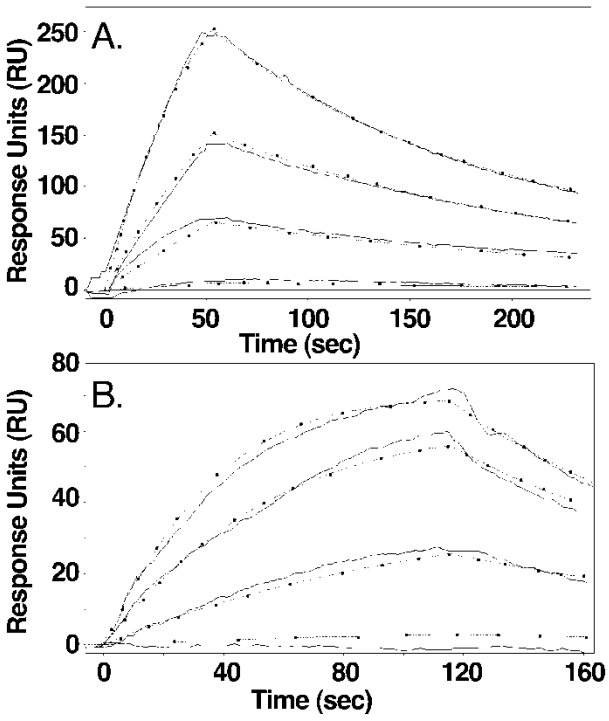

Figure 3. SPR analysis of the interaction of gambogic acid (**1**) with (A) full length Hsp90 and (B) the N-terminal domain of Hsp90. A. Injection of 1.0, 10, 25 and 50 □M **1** over a SPR chip containing bound full length Hsp90. B. Injection of 0.5, 5, 15 and 25 □M **1** over a SPR chip containing bound Hsp90NT. Black line: sensorgram of binding and dissociation; gray line: curve fit.

Table 1. Constants for the Binding of Gambogic Acid (**1**) to Hsp90

protein	k_a (M^{-1} S^{-1})	k_d (S^{-1})	K_D (μM)
full length Hsp90	1.16(8)e^3	0.0113(4)	9.8(2)
Hsp90NT	1.47(6)e^3	0.01122(7)	7.6(3)
Hsp90NT (+20μM GA)	1.62(8)e^3	0.0114(7)	7.0(4)
Hsp90CT	no binding		

REFERENCES

Albert, T.K., et al., *Identification of a ubiquitin-protein ligase subunit within the CCR4-NOT transcription repressor complex.* EMBO J, 2002. **21**(3): p. 355-64.

Anderson, P., & Kedersha, N. (2008). Stress granules: the Tao of RNA triage. *Trends in biochemical sciences*, *33*(3), 141-50. doi:10.1016/j.tibs.2007.12.003

Angers, S., Li, T., Yi, X., MacCoss, M. J., Moon, R. T., & Zheng, N. (2006). Molecular architecture and assembly of the DDB1-CUL4A ubiquitin ligase machinery. *Nature*, *443*(7111), 590-3. doi:10.1038/nature05175

Arnold, K., et al., *The SWISS-MODEL workspace: a web-based environment for protein structure homology modelling.* Bioinformatics, 2006. **22**(2): p. 195-201.

Aspenstrom, P., A. Fransson, and J. Saras, *Rho GTPases have diverse effects on the organization of the actin filament system.* Biochem J, 2004. **377**(Pt 2): p. 327-37.

Aspenström, P., Ruusala, A., & Pacholsky, D. (2007). Taking Rho GTPases to the next level: the cellular functions of atypical Rho GTPases. *Experimental cell research*, *313*(17), 3673-9. doi:10.1016/j.yexcr.2007.07.022

Barash, I., *Stat5 in the mammary gland: controlling normal development and cancer.* J Cell Physiol, 2006. **209**(2): p. 305-13.

Bement, W.M., A.L. Miller, and G. von Dassow, *Rho GTPase activity zones and transient contractile arrays.* Bioessays, 2006. **28**(10): p. 983-93.

Bennett-Lovsey, R.M., et al., *Exploring the extremes of sequence/structure space with ensemble fold recognition in the program Phyre.* Proteins, 2008. **70**(3): p. 611-25.

Berthold, J., K. Schenkova, and F. Rivero, *Rho GTPases of the RhoBTB subfamily and tumorigenesis.* Acta Pharmacol Sin, 2008. **29**(3): p. 285-95.

Berthold, J., Schenková, K., & Rivero, F. (2008). Invited review Rho GTPases of the RhoBTB subfamily and tumorigenesis. *Molecular Medicine*, *29*(3), 285-295. doi:10.1111/j.1745

Berthold, J., Schenková, K., Ramos, S., Miura, Y., Furukawa, M., Aspenström, P., & Rivero, F. (2008). Characterization of RhoBTB-dependent Cul3 ubiquitin ligase complexes--evidence for an autoregulatory mechanism. *Experimental cell research*, *314*(19), 3453-65. Elsevier Inc. doi:10.1016/j.yexcr.2008.09.005

Blom, N., et al., *Prediction of post-translational glycosylation and phosphorylation of proteins from the amino acid sequence.* Proteomics, 2004. **4**(6): p. 1633-49.

Bokatzian-johnson, S. S. (2008). Surface Plasmon Resonance : Principles and Applications. *Plasmonics*.

BostonBiochem. [cited; Available from: http://www.bostonbiochem.com/upp.php.

Boureux, A., et al., *Evolution of the Rho family of ras-like GTPases in eukaryotes.* Mol Biol Evol, 2007. **24**(1): p. 203-16.

Boureux, A., Vignal, E., Faure, S., & Fort, P. (2007). Evolution of the Rho family of ras-like GTPases in eukaryotes. *Molecular biology and evolution*, *24*(1), 203-16. doi:10.1093/molbev/msl145

Brooks, S. a. (2010). Functional interactions between mRNA turnover and surveillance and the ubiquitin proteasome system. *Wiley Interdisciplinary Reviews - RNA*, *1*(2), 240-252. doi:10.1002/wrna.11

Brown, J. M., Green, J., das Neves, R. P., Wallace, H. a C., Smith, A. J. H., Hughes, J., Gray, N., et al. (2008). Association between active genes occurs at nuclear speckles and is modulated by chromatin environment. *The Journal of cell biology*, *182*(6), 1083-97. doi:10.1083/jcb.200803174

Cayli, S., Klug, J., Chapiro, J., Fröhlich, S., Krasteva, G., Orel, L., & Meinhardt, A. (2009). COP9 signalosome interacts ATP-dependently with p97/valosin-containing protein (VCP) and controls the ubiquitination status of proteins bound to p97/VCP. The Journal of biological chemistry, 284(50), 34944-53. doi:10.1074/jbc.M109.037952

Chamovitz, Daniel, A. (2009). Revisting the COP9 signalosome as a transcriptional regulator. *EMBO reports, 10*(4), 352-358. doi:10.1038/embor.2009.33

Chang, F. K., Sato, N., Kobayashi-Simorowski, N., Yoshihara, T., Meth, J. L., & Hamaguchi, M. (2006). DBC2 is essential for transporting vesicular stomatitis virus glycoprotein. *Journal of molecular biology*, *364*(3), 302-8. doi:10.1016/j.jmb.2006.09.026

Chardin, P. (2006). Function and regulation of Rnd proteins. *Nature reviews. Molecular cell biology*, *7*(1), 54-62. doi:10.1038/nrm1788

Chen, C.Y. and W.E. Balch, *The Hsp90 chaperone complex regulates GDI-dependent Rab recycling.* Mol Biol Cell, 2006. **17**(8): p. 3494-507.

Cho, Y. G., Choi, B. J., Kim, C. J., Song, J. H., Zhang, C., Nam, S. W., Lee, J. Y., et al. (2008). Genetic analysis of the DBC2 gene in gastric cancer. *Acta oncologica (Stockholm, Sweden)*, *47*(3), 366-71. doi:10.1080/02841860701644094

Clevenger, C.V., *Roles and regulation of stat family transcription factors in human breast cancer.* Am J Pathol, 2004. **165**(5): p. 1449-60.

Collado, D., Yoshihara, T., & Hamaguchi, M. (2007). DBC2 resistance is achieved by enhancing 26S proteasome-mediated protein degradation. *Biochemical and biophysical research communications*, *360*(3), 600-3. doi:10.1016/j.bbrc.2007.06.127

Coopman, P.J., et al., *The Syk tyrosine kinase suppresses malignant growth of human breast cancer cells.* Nature, 2000. **406**(6797): p. 742-7.

Craig, D. et al. (1992) Plasmid cDNA-directed protein synthesis in a coupled eukaryotic in vitro transcription-translation system. Nucleic Acids Res. 20, 4987–95.

Daumke, O., et al., *The GTPase-activating protein Rap1GAP uses a catalytic asparagine.* Nature, 2004. **429**(6988): p. 197-201.

Davenport, J., Manjarrez, J. R., Peterson, L., Krumm, B., Blagg, B. S. J., & Matts, R. L. (2011). Gambogic Acid, a natural product inhibitor of hsp90. *Journal of natural products*, *74*(5), 1085-92. doi:10.1021/np200029q

DerMardirossian, C. and G.M. Bokoch, *GDIs: central regulatory molecules in Rho GTPase activation.* Trends Cell Biol, 2005. **15**(7): p. 356-63.

Dhordain, P. (1995). Capsule Domain : A New Protein-Protein Interaction to DNA- and Actin-binding Proteins ' The BTB / POZ Motif Common. *Cell Growth & Differentiation*, *6*(September), 1193-1198.

Echeverria, P. C., & Picard, D. (2010). Molecular chaperones, essential partners of steroid hormone receptors for activity and mobility. *Biochimica et biophysica acta*, *1803*(6), 641-9. Elsevier B.V. doi:10.1016/j.bbamcr.2009.11.012

Enchev, R. I., Schreiber, A., Beuron, F., & Morris, E. P. (2010). Structural Insights into the COP9 Signalosome and Its Common Architecture with the 26S Proteasome Lid and eIF3. *Structure/Folding and Design*, *18*(4), 518-527. Elsevier Ltd. doi:10.1016/j.str.2010.02.008

Eskew, J. D., Sadikot, T., Morales, P., Duren, A., Dunwiddie, I., Swink, M., Zhang, X., et al. (2011). *Development and characterization of a novel C-terminal inhibitor of Hsp90 in androgen dependent and independent prostate cancer cells. BMC cancer* (Vol. 11, p. 468). doi:10.1186/1471-2407-11-468

Fehon, R. G., Mcclatchey, A. I., & Bretscher, A. (2010). Organizing the cell cortex : the role of ERM proteins. *Cancer Research*, *11*(ApRIl), 276-287. Nature Publishing Group. doi:10.1038/nrm2866

Finn, R.D., et al., *Pfam: clans, web tools and services.* Nucleic Acids Res, 2006. **34**(Database issue): p. D247-51.

Fox, A. H., & Lamond, A. I. (2010). Paraspeckles. *Cold Sprin Harbor perspectives in Biology*, *June 23*. doi:10.1101/cshperspect.a000687

Fox, A. H., Lam, Y. W., Leung, A. K. L., Lyon, C. E., Andersen, J., Mann, M., & Lamond, A. I. (2002). Paraspeckles : A Novel Nuclear Domain. *Current*, *12*(01), 13-25.

Freeman, S. N., & Cress, W. D. (2010). RhoBTB2 (DBC2) comes of age as a multifunctional tumor suppressor. *Cancer biology & therapy*, *10*(11), 1123-5. Retrieved from http://www.ncbi.nlm.nih.gov/pubmed/20980811

Freeman, S. N., Ma, Y., & Cress, W. D. (2008). RhoBTB2 (DBC2) is a mitotic E2F1 target gene with a novel role in apoptosis. *The Journal of biological chemistry*, *283*(4), 2353-62. doi:10.1074/jbc.M705986200

Grenert, J. P.; Sullivan, W. P.; Fadden, P.; Haystead, T. A.;Clark, J.; Mimnaugh, E.; Krutzsch, H.; Ochel, H. J.; Schulte, T.W.;Sausville, E.; Neckers, L. M.; Toft, D. O. J. Biol. Chem. 1997,272, 23843–23850.

Hamaguchi, M., et al., *DBC2, a candidate for a tumor suppressor gene involved in breast cancer.* Proc Natl Acad Sci U S A, 2002. **99**(21): p. 13647-52.

Hanzawa, H., et al., *The structure of the C4C4 ring finger of human NOT4 reveals features distinct from those of C3HC4 RING fingers.* J Biol Chem, 2001. **276**(13): p. 10185-90.

Hartson, S. D., Barrett, D. J., Burn, P., & Matts, R. L. (1996). Hsp90-mediated folding of the lymphoid cell kinase p56lck. *Biochemistry*, *35*(41), 13451-9. doi:10.1021/bi961332c

Hori, T., et al., *Covalent modification of all members of human cullin family proteins by NEDD8.* Oncogene, 1999. **18**(48): p. 6829-34.

Johnson, B. D., Chadli, A., Felts, S. J., Bouhouche, I., Catelli, M. G., & Toft, D. O. (2000). Hsp90 Chaperone Activity Requires the Full-length Protein and Interaction among Its Multiple Domains *. *October*, *275*(42), 32499 -32507. doi:10.1074/jbc.M005195200

Kato, J.-ya, & Yoneda-Kato, N. (2009). Mammalian COP9 signalosome. *Genes to cells : devoted to molecular & cellular mechanisms*, *14*(11), 1209-25. doi:10.1111/j.1365-2443.2009.01349.x

Kedersha, N., Stoecklin, G., Ayodele, M., Yacono, P., Lykke-Andersen, J., Fritzler, M. J., Scheuner, D., et al. (2005). Stress granules and processing bodies are dynamically linked sites of mRNP remodeling. The Journal of cell biology, 169(6), 871-84. doi:10.1083/jcb.200502088

Kelly, K.F. and J.M. Daniel, *POZ for effect--POZ-ZF transcription factors in cancer and development.* Trends Cell Biol, 2006. **16**(11): p. 578-87.

Kimball, S. R., Horetsky, R. L., Ron, D., Jefferson, L. S., & Harding, H. P. (2003). Mammalian stress granules represent sites of accumulation of stalled translation initiation complexes. *American journal of physiology. Cell physiology*, *284*(2), C273-84. doi:10.1152/ajpcell.00314.2002

Knowles, M. a, Aveyard, J. S., Taylor, C. F., Harnden, P., & Bass, S. (2005). Mutation analysis of the 8p candidate tumour suppressor genes DBC2 (RHOBTB2) and LZTS1 in bladder cancer. *Cancer letters*, *225*(1), 121-30. doi:10.1016/j.canlet.2004.10.047

Kopp, J. and T. Schwede, *The SWISS-MODEL Repository of annotated three-dimensional protein structure homology models.* Nucleic Acids Res, 2004. **32**(Database issue): p. D230-4.

Kopp, J. and T. Schwede, *The SWISS-MODEL Repository: new features and functionalities.* Nucleic Acids Res, 2006. **34**(Database issue): p. D315-8.

Lee, P., Rao, J., Fliss, A., Yang, E., Garrett, S., & Caplan, A. J. (2002). The Cdc37 protein kinase-binding domain is sufficient for protein kinase activity and cell viability. *The Journal of cell biology*, *159*(6), 1051-9. doi:10.1083/jcb.200210121

Ling, Li-Jun, Lu, Chao, Zhou, Guo-Ping & Wang, Shui. (2010) Ectopic expression of RhoBTB2 inhibits migration and invasion of human breast cancer cells. *Cancer Biol Ther*. 2010 Dec 1;10(11):1115-22. PMID: 20930524

MacLean, M., & Picard, D. (2003). Cdc37 goes beyond Hsp90 and kinases. *Cell stress & chaperones*, *8*(2), 114-9. Retrieved from http://www.pubmedcentral.nih.gov/articlerender.fcgi?artid=514862&tool=pmcentrez&rendertype=abstract

Mao, H., Qu, X., Yang, Y., Zuo, W., Bi, Y., Zhou, C., Yin, H., et al. (2010). A Novel Tumor Suppressor Gene RhoBTB2 (DBC2): Frequent Loss of Expression in Sporadic Breast Cancer. *Molecular Carcinogenesis*, *289*(November 2009), 283-289. doi:10.1002/mc.20598

Mao, H., Zhang, L., Yang, Y., Sun, J., Deng, B., Feng, J., & Shao, Q. (2011). RhoBTB2 (DBC2) functions as tumor suppressor via inhibiting proliferation , preventing colony formation and inducing apoptosis in breast cancer cells. *Gene*, *486*(1-2), 74-80. Elsevier B.V. doi:10.1016/j.gene.2011.07.018

Masuda-Robens, J.M., et al., *The TRE17 oncogene encodes a component of a novel effector pathway for Rho GTPases Cdc42 and Rac1 and stimulates actin remodeling.* Mol Cell Biol, 2003. **23**(6): p. 2151-61.

McEvoy, J.D., et al., *Constitutive turnover of cyclin E by Cul3 maintains quiescence.* Mol Cell Biol, 2007. **27**(10): p. 3651-66.

McKinnon, C. M., Lygoe, K. a, Skelton, L., Mitter, R., & Mellor, H. (2008). The atypical Rho GTPase RhoBTB2 is required for expression of the chemokine CXCL14 in normal and cancerous epithelial cells. *Oncogene*, *27*(54), 6856-65. doi:10.1038/onc.2008.317

McNiven, M. A. (2011). Vesicle Formation at the Plasma The Same but Different. *Science*, *1591*(2006). doi:10.1126/science.1118133

Merwe, P. A. V. D. (n.d.). Surface plasmon resonance GENERAL PRINCIPLES OF BIACORE EXPERIMENTS, 1-50.

Miller, B. J., Wang, D., Krahe, R., & Wright, F. a. (2003). Pooled analysis of loss of heterozygosity in breast cancer: a genome scan provides comparative evidence for multiple tumor suppressors and identifies novel candidate regions. *American journal of human genetics*, *73*(4), 748-67. doi:10.1086/378522

MotifScan. [cited; Available from: http://myhits.isb-sib.ch/cgi-bin/motif_scan.

Mulder, K.W., et al., *Modulation of Ubc4p/Ubc5p-mediated stress responses by the RING-finger-dependent ubiquitin-protein ligase Not4p in Saccharomyces cerevisiae.* Genetics, 2007. **176**(1): p. 181-92.

Owen, B. A.; Sullivan, W. P.; Felts, S. J.; Toft, D. O. J. Biol. Chem.2002, 277, 7086–7091.

Paduch, M., F. Jelen, and J. Otlewski, *Structure of small G proteins and their regulators.* Acta Biochim

Pol, 2001. **48**(4): p. 829-50.

Pan, X., et al., *TBC-domain GAPs for Rab GTPases accelerate GTP hydrolysis by a dual-finger mechanism.* Nature, 2006. **442**(7100): p. 303-6.

Pearl, L. H. (2005). Hsp90 and Cdc37 -- a chaperone cancer conspiracy. *Current opinion in genetics & development*, *15*(1), 55-61. doi:10.1016/j.gde.2004.12.011

Perez-Torrado, R., D. Yamada, and P.A. Defossez, *Born to bind: the BTB protein-protein interaction domain.* Bioessays, 2006. **28**(12): p. 1194-202.

Picard, D. (2006). Chaperoning steroid hormone action. *Trends in Endocrinology and Metabolism*, *17*(6). doi:10.1016/j.tem.2006.06.003

Pintard, L., A. Willems, and M. Peter, *Cullin-based ubiquitin ligases: Cul3-BTB complexes join the family.* EMBO J, 2004. **23**(8): p. 1681-7.

Puntervoll, P., et al., *ELM server: A new resource for investigating short functional sites in modular eukaryotic proteins.* Nucleic Acids Res, 2003. **31**(13): p. 3625-30.

Ramos, S., et al., *Genomic organization and expression profile of the small GTPases of the RhoBTB family in human and mouse.* Gene, 2002. **298**(2): p. 147-57.

Rao, J., Lee, P., Benzeno, S., Cardozo, C., Albertus, J., Robins, D. M., and Caplan, A J., (2001). Functional Interaction of Human Cdc37 with the Androgen Receptor but Not with the Glucocorticoid Receptor. *Journal of Biological Chemistry,* 276, 5814-5820.

Rechsteiner, M. and S.W. Rogers, *PEST sequences and regulation by proteolysis.* Trends Biochem Sci, 1996. **21**(7): p. 267-71.

Reed, S. I. (1980). The Selection of S. Cerevzszae Mutants Defective in the Start Event of Cell Divison. *Genetics.*, *Jul;95*(3), 561-577.

Rehmann, H. and J.L. Bos, *Signal transduction: thumbs up for inactivation.* Nature, 2004. **429**(6988): p. 138-9.

Rich, R. L., & Myszka, D. G. (2008). Survey of the year 2007 commercial optical biosensor literature. *Journal of molecular recognition : JMR*, *21*(6), 355-400. doi:10.1002/jmr.928

Ricketson, D., Hostick, U., Fang, L., Yamamoto, K. R., & Darimont, B. D. (2007). A Conformational Switch in the Ligand-binding Domain Regulates the Dependence of the Glucocorticoid Receptor on Hsp90. *Receptor*, 729-741. doi:10.1016/j.jmb.2007.02.057

Roe, S. M., Ali, M. M. U., Meyer, P., Vaughan, C. K., Panaretou, B., Piper, P. W., Prodromou, C., et al. (2004). The Mechanism of Hsp90 regulation by the protein kinase-specific cochaperone p50(cdc37). *Cell*, *116*(1), 87-98. Retrieved from http://www.ncbi.nlm.nih.gov/pubmed/14718169

Rogers, S., R. Wells, and M. Rechsteiner, *Amino acid sequences common to rapidly degraded proteins: the PEST hypothesis.* Science, 1986. **234**(4774): p. 364-8.

Roiniotis, J., Masendycz, P., Ho, S., & Scholz, G. M. (2005). Domain-mediated dimerization of the Hsp90 cochaperones Harc and Cdc37. *Biochemistry*, *44*(17), 6662-9. doi:10.1021/bi047406z

Salas-Vidal, E., Meijer, A. H., Cheng, X., & Spaink, H. P. (2005). Genomic annotation and expression analysis of the zebrafish Rho small GTPase family during development and bacterial infection. *Genomics*, *86*(1), 25-37. doi:10.1016/j.ygeno.2005.03.010

Salichs, E., Ledda, A., Mularoni, L., Albà, M. M., & de la Luna, S. (2009). Genome-wide analysis of histidine repeats reveals their role in the localization of human proteins to the nuclear speckles compartment. *PLoS genetics*, *5*(3), e1000397. doi:10.1371/journal.pgen.1000397

Salinas, G.D., et al., *Actinfilin is a Cul3 substrate adaptor, linking GluR6 kainate receptor subunits to the ubiquitin-proteasome pathway.* J Biol Chem, 2006. **281**(52): p. 40164-73.

Scholz, G. M., Cartledge, K., & Hall, N. E. (2001). Identification and characterization of Harc, a novel Hsp90-associating relative of Cdc37. *The Journal of biological chemistry*, *276*(33), 30971-9. doi:10.1074/jbc.M103889200

Schwede, T., et al., *SWISS-MODEL: An automated protein homology-modeling server.* Nucleic Acids Res, 2003. **31**(13): p. 3381-5.

Seewald, M.J., et al., *RanGAP mediates GTP hydrolysis without an arginine finger.* Nature, 2002. **415**(6872): p. 662-6.

Seol, J.H., et al., *Cdc53/cullin and the essential Hrt1 RING-H2 subunit of SCF define a ubiquitin ligase module that activates the E2 enzyme Cdc34.* Genes Dev, 1999. **13**(12): p. 1614-26.

Shao, J., Irwin, A., Hartson, S. D., & Matts, R. L. (2003). Functional dissection of cdc37: characterization of domain structure and amino acid residues critical for protein kinase binding. *Biochemistry*, *42*(43), 12577-88. doi:10.1021/bi035138j

Shao, J., Prince, T., Hartson, S. D., & Matts, R. L. (2003). Phosphorylation of serine 13 is required for the proper function of the Hsp90 co-chaperone, Cdc37. *The Journal of biological chemistry*, *278*(40), 38117-20. doi:10.1074/jbc.C300330200

Shellenberger, T. D., Wang, M., Gujrati, M., Shellenberger, T. D., Wang, M., Gujrati, M., Jayakumar, A., et al. (2004). BRAK / CXCL14 Is a Potent Inhibitor of Angiogenesis and a Chemotactic Factor for Immature Dendritic Cells BRAK / CXCL14 Is a Potent Inhibitor of Angiogenesis and a Chemotactic Factor for Immature Dendritic Cells. *Design*, 8262-8270. doi:10.1158/0008-5472.CAN-04-2056

Shi, Y., Chen, J.-Y., Yang, J., Li, B., Chen, Z.-H., & Xiao, C.-G. (2008). DBC2 gene is silenced by promoter methylation in bladder cancer. *Urologic oncology*, *26*(5), 465-9. doi:10.1016/j.urolonc.2007.08.009

Shiau, A. K., Massari, M. E., & Ozbal, C. C. (2008). Back to basics: label-free technologies for small molecule screening. *Combinatorial chemistry & high throughput screening*, *11*(3), 231-7. Retrieved from http://www.ncbi.nlm.nih.gov/pubmed/18336215

Silva, C.M., *Role of STATs as downstream signal transducers in Src family kinase-mediated tumorigenesis.* Oncogene, 2004. **23**(48): p. 8017-23.

Singer, J.D., et al., *Cullin-3 targets cyclin E for ubiquitination and controls S phase in mammalian cells.* Genes Dev, 1999. **13**(18): p. 2375-87.

Siripurapu, V., Meth, J., Kobayashi, N., & Hamaguchi, M. (2005). DBC2 significantly influences cell-cycle, apoptosis, cytoskeleton and membrane-trafficking pathways. *Journal of molecular biology*, *346*(1), 83-9. doi:10.1016/j.jmb.2004.11.043

Smith, J. R., Clarke, P. a, de Billy, E., & Workman, P. (2009). Silencing the cochaperone CDC37 destabilizes kinase clients and sensitizes cancer cells to HSP90 inhibitors. *Oncogene*, *28*(2), 157-69. doi:10.1038/onc.2008.380

Stead, M.A., et al., *A beta-sheet interaction interface directs the tetramerisation of the Miz-1 POZ domain.* J Mol Biol, 2007. **373**(4): p. 820-6.

Stogios, P. J., Downs, G. S., Jauhal, J. J. S., Nandra, S. K., & Privé, G. G. (2005). Sequence and structural analysis of BTB domain proteins. *Genome biology*, *6*(10), R82. doi:10.1186/gb-2005-6-10-r82

St-Pierre, B., Jiang, Z., Egan, S. E., & Zacksenhaus, E. (2004). High expression during neurogenesis but not mammogenesis of a murine homologue of the Deleted in Breast Cancer2/Rhobtb2 tumor suppressor. *Gene expression patterns : GEP*, *5*(2), 245-51. doi:10.1016/j.modgep.2004.07.009

Thillaivinayagalingam, P., Gommeaux, J., McLoughlin, M., Collins, D., & Newcombe, A. R. (2010). Biopharmaceutical production: Applications of surface plasmon resonance biosensors. *Journal of chromatography. B, Analytical technologies in the biomedical and life sciences*, *878*(2), 149-53. doi:10.1016/j.jchromb.2009.08.040

Vadlamudi, R.K. and R. Kumar, *P21-activated kinases in human cancer.* Cancer Metastasis Rev, 2003. **22**(4): p. 385-93.

van den Heuvel, S., *Protein degradation: CUL-3 and BTB--partners in proteolysis.* Curr Biol, 2004. **14**(2): p. R59-61.

Vaughan, C. K., Mollapour, M., Smith, J. R., Truman, A., Hu, B., Good, V. M., Panaretou, B., et al. (2008). Hsp90-Dependent Activation of Protein Kinases Is Regulated by Chaperone-Targeted Dephosphorylation of Cdc37. *Molecular Cell*, *37*, 886-895. doi:10.1016/j.molcel.2008.07.021

Vlahou, G. and F. Rivero, *Rho GTPase signaling in Dictyostelium discoideum: insights from the genome.* Eur J Cell Biol, 2006. **85**(9-10): p. 947-59.

Welcker, M., et al., *Multisite phosphorylation by Cdk2 and GSK3 controls cyclin E degradation.* Mol

Cell, 2003. **12**(2): p. 381-92.

Wilkins, A., & Carpenter, C. L. (2008). Regulation of RhoBTB2 by the Cul3 ubiquitin ligase complex. *Methods in enzymology*, *439*(07), 103-9. doi:10.1016/S0076-6879(07)00408-9

Wilkins, A., Ping, Q., & Carpenter, C. L. (2004). RhoBTB2 is a substrate of the mammalian Cul3 ubiquitin ligase complex. *Genes & development*, *18*(8), 856-61. doi:10.1101/gad.1177904

Willems, A. R., Schwab, M., & Tyers, M. (2004). A hitchhiker ' s guide to the cullin ubiquitin ligases : SCF and its kin. *Biochim Biophys Acta*, *1695*, 133 - 170. doi:10.1016/j.bbamcr.2004.09.027

Wimuttisuk, W. and J.D. Singer, *The Cullin3 ubiquitin ligase functions as a Nedd8-bound heterodimer.* Mol Biol Cell, 2007. **18**(3): p. 899-909.

Yanagi, S., et al., *Syk expression and novel function in a wide variety of tissues.* Biochem Biophys Res Commun, 2001. **288**(3): p. 495-8.

Yoshihara, T., Collado, D., & Hamaguchi, M. (2007). Cyclin D1 down-regulation is essential for DBC2's tumor suppressor function. *Biochemical and biophysical research communications*, *358*(4), 1076-9. doi:10.1016/j.bbrc.2007.05.037

Zhao, J., Wang, C., Wang, J., Yang, X., Diao, N., Li, Q., Wang, W., et al. (2011). E3 ubiquitin ligase Siah-1 facilitates poly-ubiquitylation and proteasomal degradation of the hepatitis B viral X protein. *FEBS Letters*, *585*(19), 2943-2950. Federation of European Biochemical Societies. doi:10.1016/j.febslet.2011.08.015

APPENDIX A

Chemical Structures

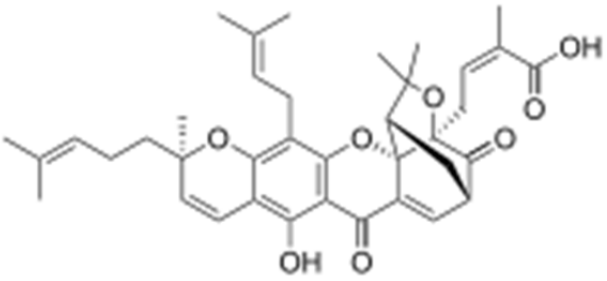

The chemical structure of Gambogic Acid (GBA) found at http://en.wikipedia.org/wiki/Gambogic_acid.

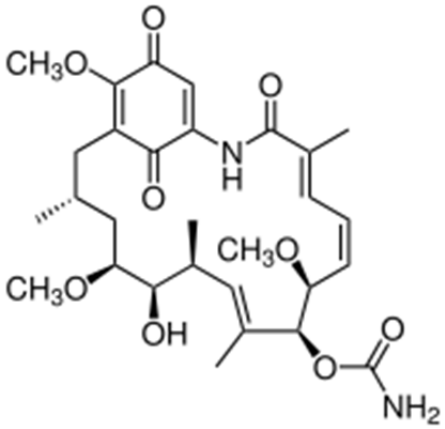

The chemical structure of Geldanamycin (GA) found at http://en.wikipedia.org/wiki/Geldanamycin.

APPENDIX B

Abbreviations

Abbreviations	Terms
^{35}S	radioactive sulfur 35
A	Adenine
AA	Amino Acid
ABC	Ammonium bicarbonate
Akt2	V-akt murine thymoma viral oncogene homolog 2
alanine	Ala, A
AP-2	Transcription factor AP-2
AP-3	Transcription factor AP-3
arginine	Arg, R
asparagine	Asn, N
aspartic acid	Asp, D
ATPase	Enzyme that cleaves ATP
BCL6	B-cell lymphoma 6 protein
BLAST	Basic Local Alignment SearchTool
BRAC2	breast cancer type 2 susceptibility protein
BRCA1	breast cancer type 1 susceptibility protein
BRMS1	Breast cancer metastasis suppressor 1
BTB/POZ	broad-complex tramtrack, bric a brac, poxvirus zinc finger
BTBk	BTB (POZ) domain contain Kelch repeat
BTB-ZF	BTB (POZ) -Zinc finger
C	Cytosine
C12orf51	Chromosome 12 open reading frame 51
Cdc32	Cell division control protein 42 homolog

cdc37	Cell division cycle 37 homolog
cdk5	Cyclin-dependent kinase 5
CKI	Casein kinase 1
CKII	Casein kinase 2
CRL	Cullin-RING E3 ligase
C-terminal	carboxylic acid terminal
Cul	cullin
CXCL14	Chemokine (C-X-C motif) ligand 14
cysteine	Cys, C
DBC2	Deleted in Breast Cancer 2
DCP2	mRNA-decapping enzyme 2
DMEM	Dulbecco/Vogt modified Eagle's minimal essential medium
DMSO	Dimethyl sulfoxide
DNA	Deoxyribonucleic acid
E.coli	Escherichia coli
E1	ubiquitin-activating enzyme
E2	ubiquitin-conjugating enzyme
E3	ubiquitin-protein ligase
EDTA	Ethylenediaminetetraacetic acid
EF2	E2F transcription factor family
ER	endoplasmic reticulum
FHA	Forkhead-associated domain
G	Guanine
G cycle	GTPase cycel
G proteins	GTPase proteins
G3BP1	Ras GTPase-activating protein-binding protein 1
GA	geldanamycin
GAP	GTPase activating proteins

GDF	GDI disassoication factor
GDI	Guanine disassoication inhibitor
GDP	guanosine diphosphate
GDP	Guanosine diphosphate
GEF	Guanine nucleotide exchange factor
glutamic acid	Glu, E
glutamine	Gln, Q
glycine	Gly, G
GMP	guanosine monophosphate
GMP	Guanosine monophosphate
GSK3	Glycogen synthase kinase 3
GTP	guanosine triphosphate
GTP	Guanosine-5'-triphosphate
GTPase	guanosine triphosphatase
GTPase	Enzyme that cleaves GTP
HECT	Homologous to the E6-AP Carboxyl Terminus domain
HeLa	"Henrietta Lacks" cervical caner- epithelial
histidine	His, H
Hop	Stress-induced-phosphoprotein 1
Hsc70	Heat shock 70 kDa protein 8
Hsp70	70 kilodalton heat shock proteins
Hsp90	Heat Shock protein 90kDa
IgG	Immunoglobulin G
isoleucine	Ile, I
K562	Lymphoblastoid
kDa	kiloDalton
KOAc	Potassium acetate
LC-MS	Liquid chromatography–mass spectrometry

LC-MS-MS	Liquid chromatography–mass spectrometry-mass spectrometry
Lck	Lymphocyte-specific protein tyrosine kinase
leucine	Leu, L
LOH	Loss of heterozygosity
lysine	Lys, K
MALDI-TOF	Matrix-assisted laser desorption/ionization-time of flight
MATH	Meprin and TRAF homology domain
MCF-7	"Michigan Cancer Foundation-7" Invasive breast ductal carcinoma
methionine	Met, M
$Mg(Oac)_2$	magnesium acetate
MG132	Z-Leu-Leu-Leu-al
Miz-1	Zinc finger and BTB domain containing 17
MoO4	molybdate
MS	mass spectrometry
N_2	Nitrogen
NaCl	sodium chloride
NCBI	National Center for Biotechnology Information
Nedd8	Neural precursor cell expressed, developmentally down-regulated 8
NLS	Nuclear localization signal
NOT4	CCR4-NOT transcription complex subunit 4
N-terminal	amino terminal
p23	Prostaglandin E synthase 3
p38MAPK	P38 mitogen-activated protein kinase
Pak1	P21 protein (Cdc42/Rac)-activated kinase 1
PCD	Programmed Cell Death
PCR	Polymerase chain reaction
pfu	DNA polymerase from the archaeon *Pyrococcus furiosus*
phenylalanine	Phe, F

PHYRE	Protein Homology/AnalogY Recognition Engine
PKC	Protein Kinase C
PLZF	Promyelocytic leukemia zinc-finger
Poly-A	Polyadenylation
ProD-kinase	Proline directed kinase 1
proline	Pro, P
psi	pounds per square inch
PSI-BLAST	Position-Specific Iterative BLAST
PVDF	Polyvinylidene fluoride
PyMOL	Molecular modeling software
Rap1	Ras-related protein 1
Rap1Gap	Rap1 GTPase-activating protein 1
Ras	Rat sarcoma
Rbx1	RING-Box protein 1
RDA	Representational Difference Analysis
Rho	Ras homology
RhoH	Ras homolog gene family, member H
RhoU	Ras homolog gene family, member U
RING	Really interesting new gene
Rnd1	Rho family GTPase 1
Rnd3	Rho family GTPase 1
rpm	rotations per minute
RRL	Rabbit reticulocyte lysate
SDS-PAGE	sodium dodecyl sulfate polyacrylamide gelelectrophoresis
serine	Ser, S
Skp1	S-phase kinase-associated protein 1
SOCS	suppressor of cytokine signaling
SRC	sarcoma, Proto-oncogene tyrosine-protein kinase

T	Thymine
T-47D	Breast ductal carcinoma
T7	T7 RNA polymerase from the T7 bacteriophage
TBC	tre-2/USP6, BUB2, cdc16 domain
threonine	Thr, T
TIA-1	Nucleolysin TIA-1 isoform p40
TnT	Coupled trasncription translation
tryptophan	Trp, W
tyrosine	Tyr, Y
UBE	Ubiquitin binding entity
UPS	Ubiquitin/26S proteasome pathway
UTR	untranslated region
valine	Val, V
VSVG	Vesicular stomatitis virus glycoprotein
WASP	Wiskott–Aldrich Syndrome Protein
WCL	whole cell lysate

APPENDIX C

PCR primers

Primer Name	Primer Sequence
CACC Flag Link	5' - CACCATGGACTACAAGGACGACGATGACAAGAACACCGGCGCGGCG - 3'
CACC Link DBC2	5' - CACCGGCGCGGCATGGATTCTGACATGGATTATGAAAGG - 3'
DBC2 NΔ207 CACC	5' - CACCGGCGCGGCGATGCTCATCTCCCGCCGCCACCT - 3'
DBC2 NΔ258CACC	5' - CACCGGCGCGGCGATGCACCTCCTGGAGGACCCGCTC - 3'
DBC2 NΔ297CACC	5' - CACCGGCGCGGCGATGCTCATGGACCTGAGTGAGGGGGA - 3'
DBC2 NΔ319CACC	5' - CACCGGCGCGGCGATGCACCAGGGCCACTCTGATCAA - 3'
DBC2 NΔ335CACC	5' - CACCGGCGCGGCGATGGGGCGAGACTTCCTGCTCCGA - 3'
DBC2 NΔ421CACC	5' - CACCGGCGCGGCGATGCAGCCGGGGCCCTTCCGGGCT - 3'
DBC2 NΔ470CACC	5' - CACCGGCGCGGCGATGGAGGCCTTCATGAACCAGGAGATC - 3'
DBC2 NΔ501CACC	5' - CACCGGCGCGGCGATGGTGACCTTCATCCTGGATGAT - 3'
DBC2 NΔ593CACC	5' - CACCGGCGCGGCGATGACAGTGACCGGGCTGATGGAAGC - 3'
DBC2 NΔ675CACC	5' - CACCGGCGCGGCGATGGATCATTACCAGCGGGCAC - 3'
DBC2 Nt Back	5' - TCAGACCACAGCCGAGGAGGAAGATGGGGATGA - 3'
DBC2_QC C559Y for	5' - GCCGTGCTGGAATACCTCTACACCGGCATGTTCACCTCC - 3'
DBC2_QC C559Y back	5' - GGAGGTGAACATGCCGGTGTAGAGGTATTCCAGCACGGC - 3'
DBC2_QC G99R for	5' - GCTTTGCTTATGGGAGATCTGATGTGGTGG - 3'
DBC2_QC G99R back	5' - CCACCACATCAGATCTCCCATAAGCAAAGC - 3'
D2 CΔ210 UAG top	5' - CGAGCTGCACTCATCTCCTAGCGCCACCTGCAGTTCTGG - 3'
D2 CΔ210 UAG bottom	5' - CCAGAACTGCAGGTGGCGCTAGGAGATGAGTGCAGVTCG - 3'
pcDNA3.1 HisΔ top	5' - GGTCTCGATTCTACGTGAACCGGTCATCATCACCAT - 3'
pcDNA3.1 HisΔ bottom	5' - ATGGAGATGATGACCGGTTCACGTAGAATCGAGACC - 3'
top DBC2 QC266(2) stop	5' - CTGGAGGACCCGCTCTGCTAGGACGTCATCCTGGTGCTG - 3'
bottom DBC2 QC266(2) stop	5' - CAGCACCAGGATGACGTCCTAGCAGCGCGGGTCCTCCTG - 3'

I191V top	5' - CCCTACTATGAGACCAGCGTGAGGGCCCAGTTCGGCATCAAGGACGTC - 3'
I191V bottom	5' - GACGTCCTTGATGCCGAACTGGGCCCTCACGCTGGTCTCATAGTAGGG - 3'
Rho_V191I Top 2	5' - CCCTACTATGAGACCAGCGTGATAGCCCAGTTCGGCATCAAGGAC - 3'
Rho_V191I bottom 2	5' - GTCCTTGATGCCGAACTGGGCTATCACGCTGGTCTCATAGTAGGG - 3'
Rho_V191I Top.3	5' - CATCCCCTACTATGAGACCAGCGTG ATCGCCCAGTTCGGCATCAAGGACGTC - 3'
Rho_V191I bottom.3	5' - GACGTCCTTGATGCCGAACTGGGCGATCACGCTGGTCTCATAGTAGGGGATG - 3'
I191M top	5' - CCCTACTATGAGACCAGCGTGATGGCCCAGTTCGGCATCAAGGACGTC - 3'
I191M bottom	5' - GACGTCCTTGATGCCGAACTGGGCCATCACGCTGGTCTCATAGTAGGG - 3'
I191K top	5' - CCCTACTATGAGACCAGCGTGAAGGCCCAGTTCGGCATCAAGGACGTC - 3'
I191K bottom	5' - GACGTCCTTGATGCCGAACTGGGCCTTCACGCTGGTCTCATAGTAGGG - 3'
Q141K top	5' - GACCCTGTCATCTTGGTGGGCTGAAGTTGGACCTGCGCTACGCTGACCTGGAGGCTGTC - 3'
Q141K bottom	5' - GACAGCCTCCAGGTCAGCGTAGCGCAGGTCCAACTTGCAGCCCACCAAGATGACAGGGTC - 3'
Q141R top	5' - GCACCTGTCATCTTGGTGGGCTGCCGGTTGGACCTGCGCTACGCTGACCTGGAGGCTGTC - 3'
Q141R bottom	5' - GACAGCCTCCAGGTCAGCGTAGCGCAGGTCCAACCTGCAGCCCACCAAGATGACAGGGTC - 3'
S189K top	5' - GGGCATCCCCTACTATGAGACCAAGGTGGTGGCCCAGTTCGGCATCAAGGACGTC - 3'
S189K bottom	5' - GACGTCCTTGATGCCGAACTGGGCCACCACctGGTCTCATAGTAGGGGATGCCC - 3'
S189R top	5' - GGGCATCCCCTACTATGAGACCAGGGTGGTGGCCCAGTTCGGCATCAAGGACGTC - 3'
S189R bottom	5' -GACGTCCTTGATGCCGAACTGGGCCACCACCCTGGTCTCATAGTAGGGGATGCCC - 3'
f-DBC2 T7 PCR forward	5' - GAGAGAGATAATACGACTCACTATAGGAGACGCCACCATGGACTACAAGGACGACGATGACAAG - 3'
f-DBC2 T7 PCR reverse	5' - TTTTTTTTTTTTTTTTTTTTTTTTTTTTTTTTTCAGACCACAGCCGAGGAGGAAGATGGGGATG - 3'
DBC2 Rho forward	5' - CACCATGGATTCTGACATGGATTATGAA - 3'
DBC2 Rho reverse	5' - GGAGATGAGTGCAGCTCGG - 3'
D2 S251A top	5' - CCCTCCTCGCTGGCGGAGGGAGGGTC - 3'
D2 S251A bottom	5' - GACCCTCCCTCCGCCAGCGAGGAGGG - 3'
D2 S250A top	5' - CGACCCTCCCGCCAGCAGCGAGGAG - 3'
D2 S250A bottom	5' - CTCCTCGCTGCTGGCGGGAGGGTCG - 3'
D2 K673R top	5' - CCTGTGTGGTACCTGAGGGAGGAAGATCATTACCAG - 3'
D2 K673R bottom	5' - CTGGTAATGATCTTCTCTCCTCAGGTACCACACAGG - 3'

D2 K673R top2	5' - GGCCACCTGTGTGGTACCTGAGGGAGGAAGATCATTACCAGCGGGC - 3'
D2 K673R bottom2	5' - GCCCGCTGGTAATGATCTTCCTCCCTCAGGTACCACACAGGGGTCC - 3'
D2 K673R top3	5' - CGGTGGCCACCTGTGTGGTACCTGCGCGAGGAAGATCATTACCAGCGGGCACGG - 3'
D2 K673R bottom3	5' - CCGTGCCCGCTGGTAATGATCTTCCTCGCGCAGGTACCACACAGGGGTCCACCG - 3'
D2 CΔ470 top	5' - GTGGCCAACATTCTCAACAATTAGGCCTTCATGAACCAG - 3'
D2 CΔ470 bottom	5' - CTCCTGGTTCATGAAGGCCTAATTGTTGAGATTGTTGGC - 3'
D2 CΔ470 top 2	5' - GATGGTGGCCAACATTCTCAACAATTAGGCCTTCATGAACCAGGAG - 3'
D2 CΔ470 bottom 2	5' - CTCCTGGTTCATGAAGGCCTAATTGTTGAGAATGTTGGCCACCATC - 3'
D2 CΔ600 top	5' - GTGACCGGGCTGATGTGAGCGACCCAGATGATGGTG - 3'
D2 CΔ600 bottom	5' - CACCATCATCTGGGTCGCTCACATCAGCCCGGTCAC - 3'
D2 CΔ600 top 2	5' - CACAGTGACCGGGCTGATGTGAGCGACCCAGATGATGGTGGAC - 3'
D2 CΔ600 bottom 2	5' - GTCCACCATCATCTGGGTCGCTCACATCAGCCCGGTCACTGTG - 3'
D2 CΔ210 top	5' - GCTGCACTCATCTCCTGACGCCACCTGCAG - 3'
D2 CΔ210 bottom	5' - CTGCAGGTGGCGTCAGGAGATGAGTGCAGC - 3'
HindIII-Flag_link	5' - CTAGTTAAGCTTGGATGGACTACAAGGACGACGATGACAGG - 3'
XbaI-D2-I191V-back	5' - CCCTCTAGACTCGTCAGACCACAGCCGAGGAGGAAGATG - 3'
For.DBC2 QΔ266.STOP	5' - CTGGAGGACCCGCTCTGCTAGGACGTCATCCTGGTGCTG - 3'
Rev.DBC2 QΔ266.STOP	5' - GACCTCCTGGGCGAGACGATCCTGCAGTACGACCACGAC - 3'
DBC2 NΔ210.cacc	5' - CACCGGCGCGGCGATGATCCCGCCGCCACCTGCAGTTCT - 3'
DBC2 CΔ 469 top	5' - GGCCAACATTCTCAACTAATGAGGCCTTCATGAACCAGG - 3'
DBC2 Cdelta 469 bottom	5' - CCGGTTGTAAGAGTTGATTACTCCGGAAGTACTTGGTCC - 3'
DBC2 NΔ210.cacc	5' - CACCGGCGCGGCGATGATCCCGCCGCCACCTGCAGTTCT - 3'
DBC2 NΔ500.cacc	5' - CACCGGCGCGGCGATGTCAGATGTGACCTTCATCCTGGATG - 3'
D2 CΔ 210 uaa Top	5' - CGAGCTGCACTCATCTCCTAGCGCCACCTGCAGTTCTGG - 3'
D2 CΔ 210 uaa Bottom	5' - CCAGAACTGCAGGTGGCGCTAGGAGATGAGTGCAGCTCG - 3'
D2 L300V top	5' - GACCTGTTCCTCATGGACGTGAGTGAGGGGGAG - 3'
D2 L300V bottom	5' - CTCCCCCTCACTCACGTCCATGAGGACCAGGTC - 3'
DBC2 Ring forward	5' - CACCATGGTGGACATCGATGGGGACGTC - 3'

DBC2 Ring reverse	5' - CCGTGCCCGCTGGTAATGATCTTC - 3'
DBC2 CACC topo 151	5' - CACCATGGATTCTGACATGGATTATGAAAGG - 3'
DBC2 back topo 151	5' - TCAGACCACAGCCGAGGAGGAAGATG - 3'
pSP64T f-DBC2 HindIII for	5' - GACAAGCTTATGGACTACAAGGACGACGATGACAAGAACACC - 3'
pSP64T f-DBC2 BamHI back	5' - GCGGGATCCTCAGACCACAGCCGAGGAGGAAGATG - 3'
DBC2 TA TOPO for	5' - ATGGATTCTGACATGGATTATGAAAGG - 3'
DBC2 no stop back topo/TA	5' - CCAGACCACAGCCGAGGAGGAAGATG - 3'

VITA

Jacob Ray Manjarrez

Candidate for the Degree of

Doctor of Philosophy

Thesis: FUNCTIONAL MODULATION OF DBC2 BY THE MOLECULAR CHAPERONE HSP90

Major Field: Biochemistry & Molecular Biology

Biographical:

Education:

Completed the requirements for the Doctor of Philosophy in Biochemistry & Molecular Biology at Oklahoma State University, Stillwater, Oklahoma in December, 2011.

Completed the requirements for the Bachelor of Science/Arts Cell & Molecular Biology at Oklahoma State University, Stillwater, Oklahoma in December, 2003.

Experience:

Research Associate, Professor Robert L. Matts, Oklahoma State University, Stillwater OK, Fall 2004 – Present

Teaching Associate, Dept. Zoology, Oklahoma State University, Stillwater OK, Spring 2004

Graduate Fellow, Alfred P. Sloan Foundation, Spring 2004 – Fall 2011

Graduate Fellow, OK-LSAMP Bridge to the Doctorate, Fall 2004 – Fall 2011

Undergraduate Student Researcher, Assistant/Associate Professor Gilbert H. John, Oklahoma State University, Stillwater, OK, Spring 2000 – Fall 2003

Professional Memberships:

AAAS - American Association for the Advancement of Science

Name: Jacob Ray Manjarrez Date of Degree: May, 2012

Institution: Oklahoma State University Location: Stillwater, Oklahoma

Title of Study: Functional Modulation of the DBC2 by the Molecular Chaperone Hsp90

Pages in Study: 86 Candidate for the Degree of Doctor of Philosophy

Major Field: Biochemistry and Molecular Biology

Scope and Method of Study:

This study involved looking at various mechanistic assoications of the tumor suppressor DBC2 with the Hsp90 chaperone machine. Along with aspects of functional relationships of co-chaperone and inhibitors of the Hsp90 Chaperone machine. Techniques that were used in this study include: In vitro coupled transcription/translation, Immunoprecipitation, LC-MS/MS, Tyrosine kinase assay, and Surface plasmon resonance.

Findings and Conclusions:

The tumor suppressor DBC2 was shown to be a client protein of the Hsp90 chaperone machine. The Hsp90 chaperone machine was idenitified to modulate the GTP binding of DBC2 as well as the associating protein complexes. This allowed for the detection of the protein complexes that are associated with DBC2 in resistant (HeLa) and sensitive (MCF-7) cell lines.

Additionally, this allowed for the identification of a novel Cdc37 null In vitro system in WGL. Along with the observations for direct interaction of Hsp90 with novel small molecule inhibitors

ADVISER'S APPROVAL: Dr. Robert L. Matts